Malaysian Journal of Mathematical Sciences 19(2): 411–441 (2025)
https://doi.org/10.47836/mjms.19.2.04

Malaysian Journal of Mathematical Sciences

Journal homepage: https://mjms.upm.edu.my

Global Stability and Sensitivity Analysis of SIAR Model with Influenza A (H1N1)

Sirijampa, A.* [1], Saksurakan, C. [1,2], and Janreung, S.* [1]

[1]*Division of Mathematics, Department of Social and Applied Science, College of Industrial Technology, King Mongkut's University of Technology North Bangkok, 1518 Pracharat 1 Road, Wongsawang, Bangsue, Bangkok, 10800, Thailand*
[2]*Center of Sustainable Energy and Engineering Materials (SEEM), College of Industrial Technology, King Mongkut's University of Technology North Bangkok, 1518 Pracharat 1 Road, Wongsawang, Bangsue, Bangkok, 10800, Thailand*

E-mail: aekabut.s@cit.kmutnb.ac.th
sutawas.j@cit.kmutnb.ac.th
**Corresponding author*

Received: 23 March 2024
Accepted: 19 August 2024

Abstract

The SIAR model with symptomatic and asymptomatic individuals is introduced. The stability of equilibrium points are analyzed with the basic reproduction number (R_0). The Disease-Free Equilibrium (DFE) is globally stable when $R_0 < 1$, and the Endemic Equilibrium (EE) is locally asymptotically stable when $R_0 > 1$. For case $\alpha = 0$, the global stability of EE is analyzed by using a geometric approach for the global stability. The Sensitivity Analysis (SA) of R_0 and EE with parameters of influenza A (H1N1) are presented. The most sensitive parameter for R_0 is the transmission rate to symptomatic infected individuals. The sensitivity of EE shows that the recovery rate of symptomatic and asymptomatic individuals have an effect on reducing patients when the recovery rate are increased. Therefore, controlling the spread of disease and reducing the treatment time can reduce the number of infected individuals. Simulations results by using numerical method are used to confirm the stability of the model. Further, this model is applied to predict the trend of influenza A cases of (H1N1) in Thailand during $2016 - 2022$.

Keywords: basic reproduction number; global stability; sensitivity; SIAR model analysis.

1 Introduction

Researchers employ systems of differential equations to precisely describe the behavior of natural phenomena. Since these models can predict the number of infected individuals, they play a vital role in epidemiology for investigation of disease spread and managing outbreaks. In epidemiology, there are several types of mathematical models depending on compartments and their interactions. For example, Xuhui et al. [33] constructed the SEIAR model to forecast and reproduce influenza A (H1N1) dynamics in Guangdong China. Siyu et al. [19] used the SVEIR model to fit real data on tuberculosis in China. Ratti and Kalra [31] developed a model that examines the interaction and dynamics between malaria and rotavirus, while also determining the sensitivity indices of the impact parameters. Haque et al. [10] constructed a mathematical model to investigate the transmission dynamics of Marburg virus disease. Cooper et al. [8] used the SIR model to predict the COVID-19 spreading and compare it with real data in 2020. Annas et al. [3] used the SEIR model with vaccination and isolation to study the effect of vaccine COVID-19 in Indonesia. Samuel et al. [27] used the SEIR model to predict the dynamics of COVID-19. Additionally, they considered the presence of pathogens in the environment and the impact of interventions.

The influenza A virus started its transmission in the North America in April 2009 and rapidly spread around worldwide. In June 2009, the World Health Organization classified it as a pandemic after they discovered confirmed cases in 74 countries [35]. In Thailand [29], the first cases of the pandemic were in May 2009, followed by a widespread outbreak in June. According to the 2009 surveillance report, there were $30,956$ cases, which corresponds to a prevalence rate of 48.78 per thousand people. There were 157 deaths, corresponding to a death rate of 0.31 per one thousand. Additionally, there was a 0.64 induced death rate. The majority of cases occurred between June and September, which coincides with the rainy season.

The weekly disease forecast from the Department of Disease Control in Thailand [23, 26] reports that there is an outbreak of influenza A (H1N1) in Thailand, where most patients are children aged $0-15$ years. Influenza A viruses are the only influenza viruses known to cause global epidemics of flu disease. Especially, influenza A (H1N1) virus that emerged in the spring of 2009 and cause a flu pandemic which continued to circulate seasonally [5]. Influenza has undergone extensive study and has been extensively researched. Mohamed et al. [1] used a fractional order model, which is greater to an integer-order model, to analyze the progress of influenza in Saudi Arabia over a 40 weeks period in 2017. Faizunneasa [13] used optimal control to find strategies for reducing the exposed and infected individuals in the influenza model with preventive measures and treatment interventions. Jagan [11] performed a study on the impact of vaccination on the H1N1 (A) model and determined that it is a very effective approach for minimizing the propagation of the virus. Kim et al. [14] executed an investigation on the influence of the media on the flu epidemic by analyzing data from the 2009 influenza in Korea. The results demonstrated an association between media influence and influenza, indicating that increased exposure to media lead to a decrease in the number of cases. Kanyiri et al. [12] examined the influenza model in relation to the emergence of drugs resistance. The model's findings indicate that vaccination effectively minimizes the transmission of the illness. Furthermore, using social distancing measures may serve as a control tool for reducing the occurrence of mutations in the wild-type strain.

From diagnosis, influenza patients can spread the virus 1 day before symptoms appear and continue to spread the virus $5-7$ days after signs appear in adults. Young children and people with weakened immune systems may be an infectious period of more than 7 days. People who have been exposed to the influenza virus but are asymptomatic might still transmit it during that period [6, 25]. Therefore, adding a population of asymptomatic infected individuals makes the model more consistent with reality.

In mathematical models, the SA is a frequently used method for assessing the impact of factors on the desired outcome. It is used to identify the factors that have the most significant influence on an epidemic in order to prevent an outbreak. Sensitivity analysis of the epidemic models has been used in several studies. For example, Nakul et al. [7] used SA to evaluate the comparative significance of model parameters in relation to the prevalence and transmission of malaria. Samsuzzoha et al. [32] used sensitivity analysis to find parameters that have the greatest effect on increasing R_0 and endemic equilibrium, which reduced the spread of the influenza epidemic. Sensitivity analysis was used by Rangkuti et al. [30] to find out how different factors affect the value of R_0 and the endemic equilibrium of the COVID-19 SEIR model. Al-Zahrani et al. [2] used sensitivity analysis with the SITR model to forecast the COVID-19 transmission. Abdul et al. [22] used sensitivity analysis for the COVID-19 model with quarantine and vaccination and showed that transmission of disease can be controlled by raising awareness of quarantine and vaccination in the population.

In this research, a SIAR model with symptomatic and asymptomatic infected individuals with constant immigration is introduced. Further, a transmission rate from asymptomatic to symptomatic class is added to the model. Global stability of the DFE is analyzed. A geometric approach for the global stability [20] is applied for analyzing the global stability of the endemic equilibrium. Sensitivity analysis with parameters for influenza A (H1N1) in Thailand is used to determine the most sensitive parameter for the basic reproduction number and the prevalence of the EE in order to find preventing or controlling measure for influenza A (H1N1) in the future.

2 Model Formulation

In this research, we introduce the SIR model, in which infected individuals are divided into two groups: symptomatic and asymptomatic. Thus the model consist of four types of individuals at time t: susceptible individuals $(S(t))$, symptomatic infected individuals $(I(t))$, asymptomatic infected and partially infected individuals $(A(t))$ and recovered individuals $(R(t))$. Further, the total of individuals is $N(t) = S(t) + I(t) + A(t) + R(t)$.

The number of susceptible is increased by birth or immigration, occurring at a recruitment rate denoted as Π. The number of these individuals decreases by natural death rate denoted as μ. It is hypothesized that susceptible individuals may get infected by entering into contact with symptomatic and asymptomatic individuals at rates denoted as β_I and β_A, respectively. Thus, the transmission rate to susceptible individuals is given by,

$$\frac{\beta_I I + \beta_A A}{N},$$

where β_I and β_A represent the mean number of interactions between symptomatic and asymptomatic infected individuals and susceptible individuals that are essential to disease transmission per infected individual per unit of time. Changing the number of susceptible individuals versus the time represented by,

$$\frac{dS}{dt} = \Pi - \frac{\beta_I I + \beta_A A}{N} S - \mu S. \tag{1}$$

The number of symptomatic infected individuals increased by a rate of $p(\beta_I I + \beta_A A)/N$ from contact between susceptible and infected individuals, where p is the proportion of susceptible individuals who progress to become symptomatic infected individuals. Further, I increases when asymptomatic individuals A turn symptomatic at rate σ. In addition, the variable I diminishes

due to recovery, natural death, and disease-induced death with rates γ_I, μ, and α, respectively. This gives,

$$\frac{dI}{dt} = p\frac{\beta_I I + \beta_A A}{N}S + \sigma A - (\mu + \gamma_I + \alpha)I. \tag{2}$$

The number of asymptomatic infected individuals A increases by infection of susceptible individuals at rate $(1-p)(\beta_I I + \beta_A A)/N$. Moreover, A decreases via natural death, recovery, and turning into symptomatic infected at rates μ, γ_A, and σ, respectively. Differential equations explain the relationship between the rate of change of the number of asymptomatic individuals, given by,

$$\frac{dA}{dt} = (1-p)\frac{\beta_I I + \beta_A A}{N}S - (\mu + \gamma_A + \sigma)A. \tag{3}$$

Finally, we assume that all individuals acquire permanent immunity after recovery. The number of recovered individuals, denoted as R, is increased by the rate at which symptomatic and asymptomatic infected individuals recovered, represented by γ_I and γ_A, respectively. It decreases via natural death at rate μ, so that,

$$\frac{dR}{dt} = \gamma_I I + \gamma_A A - \mu R. \tag{4}$$

All variables in this model, designed to observe human behavior, are non-negative. Further, all parameters are positive. In addition, the sum of (1)−(4) is determined,

$$\frac{dN}{dt} = \Pi - \mu N - \alpha I. \tag{5}$$

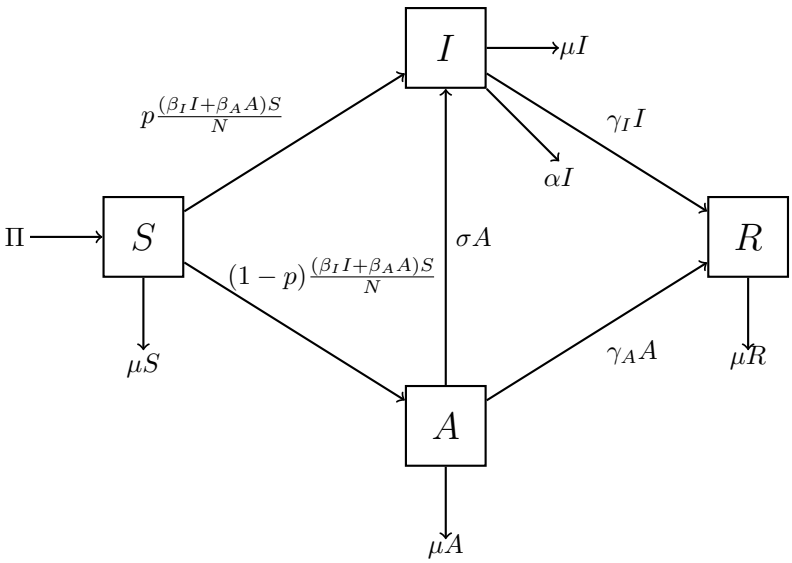

Figure 1: Diagram of SIAR model.

The transmission dynamics of the model are obvious, as shown in Figure 1. Thus, the system

of differential equations for this research is,

$$\begin{aligned}\frac{dS}{dt} &= \Pi - \frac{\beta_I I + \beta_A A}{N} S - \mu S,\\ \frac{dI}{dt} &= p\frac{\beta_I I + \beta_A A}{N} S + \sigma A - (\mu + \gamma_I + \alpha) I,\\ \frac{dA}{dt} &= (1-p)\frac{\beta_I I + \beta_A A}{N} S - (\mu + \gamma_A + \sigma) A,\\ \frac{dR}{dt} &= \gamma_I I + \gamma_A A - \mu R.\end{aligned} \tag{6}$$

The following basic property holds.

Lemma 2.1. *The closed set,*

$$\Omega = \left\{ (S, I, A, R) \in \mathbb{R}^4_+ : 0 \leq S + I + A + R \leq \frac{\Pi}{\mu} \right\},$$

is positively invariant.

Proof. The positive invariant set of the Model (6) is analyzed. Consider (5), $dN/dt \leq \Pi - \mu N$, it follows that $dN/dt \leq 0$ if $N \geq \Pi/\mu$. Thus,

$$N(t) \leq \frac{\Pi}{\mu} + \left[N(0) - \frac{\Pi}{\mu} \right] e^{-\mu t}.$$

It can be observed that $N(t) \leq \Pi/\mu$ is the case if $N(0) \leq \Pi/\mu$ and $N \to \Pi/\mu$ for all $t \to \infty$. Therefore, the area Ω is positively invariant. Moreover, if the initial value $N(0)$ is greater than Π/μ, then the solution either reaches the region Ω within a limited amount of time or the value of $N(t)$ approaches Π/μ gradually over time. Thus, all solutions in R^4_+ are attracted to the area Ω. □

3 Stability Analysis of Model

3.1 Stability of disease-free equilibrium

The disease-free equilibrium (DFE) of Model (6) is determined by setting the rate of change to zero. It is expressed as,

$$\mathcal{E}_0 = (S_0, I_0, A_0, R_0) = \left(\frac{\Pi}{\mu}, 0, 0, 0 \right).$$

In order to determine the stability of $\mathcal{E}_0$, the Jacobian matrix of the linearized model at $\mathcal{E}_0$ is computed as follows,

$$J_0 = \begin{bmatrix} -\mu & -\beta_I & -\beta_A & 0 \\ 0 & p\beta_I - k_1 & p\beta_A + \sigma & 0 \\ 0 & (1-p)\beta_I & (1-p)\beta_A - k_2 & 0 \\ 0 & \gamma_I & \gamma_A & -\mu \end{bmatrix},$$

where $k_1 = \mu + \alpha + \gamma_I$ and $k_2 = \mu + \sigma + \gamma_A$. Two eigenvalues of J_0 are $\lambda_1, \lambda_2 = -\mu$ and roots of

$$\lambda^2 + a_1 \lambda + a_2 = 0, \tag{7}$$

where

$$\begin{aligned} a_1 &= -(1-p)\beta_A - p\beta_I + k_1 + k_2, \\ &= -(k_1+k_2)(R_0-1) + \frac{(1-p)(\beta_I\sigma + \beta_A k_1)}{k_2} + \frac{p\beta_I k_2 + (1-p)\beta_I\sigma}{k_1}, \\ a_2 &= -(1-p)\beta_A k_1 - p\beta_I k_2 - (1-p)\beta_I\sigma + k_1 k_2', \\ &= -k_1 k_2(R_0-1), \end{aligned}$$

when

$$R_0 = \frac{p\beta_I k_2 + (1-p)(\beta_I\sigma + \beta_A k_1)}{k_1 k_2}. \tag{8}$$

Obviously that if $R_0 < 1$, then $a_1, a_2 > 0$ and (7) have negative real roots. Moreover, (7) has real roots which are positive in number when $R_0 > 1$, and the subsequent lemma is demonstrated.

Lemma 3.1. *The disease-free equilibrium $\mathcal{E}_0$ is locally asymptotically stable in Ω when $R_0 < 1$. Conversely, it is unstable when $R_0 > 1$.*

R_0 in (8) is called the basic reproduction number of infection. In the field of epidemiological modeling, when R_0 is less than 1, it indicates that the disease-free equilibrium is locally asymptotically stable. Specifically, if the initial sizes of the four state variables are sufficiently close to $\mathcal{E}_0$, the disease will go extinct. If the equilibrium $\mathcal{E}_0$ is globally asymptotically stable, then the illness will go extinct irrespective of the starting size of the four state variables. Thus, only the global stability of $\mathcal{E}_0$ can guarantee elimination of the disease from any stages.

3.1.1 Global stability of $\mathcal{E}_0$

Following Theorem 3.1 of [16], we prove the global stability of $\mathcal{E}_0$.

Theorem 3.1. *The disease-free equilibrium $\mathcal{E}_0$ is globally asymptotically stable in Ω if $R_0 \leq 1$, conversely, if $R_0 > 1$, then $\mathcal{E}_0$ is unstable, i.e., only solutions of (6) starting on the invariant $S-$axis approach $\mathcal{E}_0$. Otherwise, solutions move away from $\mathcal{E}_0$.*

Proof. The global stability of $\mathcal{E}_0$ is analyzed by considering the Lyapunov function which is positive definite function about $\mathcal{E}_0$,

$$V = \frac{\beta_I}{k_1} I + \left(\frac{\beta_A k_1 + \beta_I\sigma}{k_1 k_2}\right) A.$$

The derivative of V with respect to the solution of the system (6) can be expressed as,

$$\begin{aligned} V' &= \frac{\beta_I}{k_1}\left(p\frac{\beta_I I + \beta_A A}{N}S + \sigma A - k_1 I\right) + \left(\frac{\beta_A k_1 + \beta_I\sigma}{k_1 k_2}\right)\left((1-p)\frac{\beta_I I + \beta_A A}{N}S - k_2 A\right) \\ &\leq \frac{\beta_I}{k_1}\left(p(\beta_I I + \beta_A A) + \sigma A - k_1 I\right) + \left(\frac{\beta_A k_1 + \beta_I\sigma}{k_1 k_2}\right)\left((1-p)(\beta_I I + \beta_A A) - k_2 A\right) \\ &= (\beta_I I + \beta_A A)\left(p\frac{\beta_I}{k_1} + (1-p)\frac{\beta_A k_1 + \beta_I\sigma}{k_1 k_2}\right) + \frac{\beta_I\sigma}{k_1}A - \beta_I I - \left(\frac{\beta_A k_1 + \beta_I\sigma}{k_1}\right)A \\ &= (\beta_I I + \beta_A A)(R_0 - 1). \end{aligned}$$

Consequently, if $R_0 \leq 1$, then V' is less than or equal to zero, and V' is equal to zero if and only if both I and A are equal to zero. When substituting $I = A = 0$ into the first and fourth equations in (6), we get $S \to \Pi/\mu$ and $R \to 0$ as $t \to \infty$, respectively. Thus, the largest compact invariant set in $\{(S, I, A, R) \in \Omega : V' = 0\}$ is the singleton $\{\mathcal{E}_0\}$. Therefore, by the Lasalle-Lyapunov theorem ([15], Chapter 2, Theorem 6.4), as $t \to \infty$, any solution of (6) with initial sizes in Ω converges to $\mathcal{E}_0$, which corresponds to $\mathcal{E}_0$ is globally asymptotically stable in Ω when $R_0 < 1$.

Except in the case when $I = A = 0$, $V' > 0$ and S are sufficiently near to Π/μ if $R_0 > 1$. Solutions that begin sufficiently close to $\mathcal{E}_0$ exit from the neighborhood of $\mathcal{E}_0$, with the exception of those on the invariant $S-$axis, which reduces to $S' = \Pi - \mu S$, and consequently, $S(t) \to \Pi/\mu$ as $t \to \infty$ (6). This concludes the proof. □

3.2 Stability of endemic equilibrium

This section demonstrates the stability of the endemic equilibrium. The endemic equilibrium of the model (6) expressed as $\mathcal{E}^* = (S^*, I^*, A^*, R^*)$ is given by solving the model at steady-state,

$$\begin{aligned} S^* &= \frac{\Pi}{\lambda^* + \mu}, & I^* &= \frac{p\lambda^* S^* + \sigma A^*}{k_1}, \\ A^* &= \frac{(1-p)\lambda^* S^*}{k_2}, & R^* &= \frac{\gamma_I I^* + \gamma_A A^*}{\mu}, \end{aligned} \tag{9}$$

where

$$\lambda^* = \frac{\beta_I I^* + \beta_A A^*}{S^* + I^* + A^* + R^*}. \tag{10}$$

For computational feasibility, A^*, I^* and R^* in (9) are rewritten in term of $\lambda^* S^*$ as follows:

$$\begin{aligned} A^* &= \frac{(1-p)\lambda^* S^*}{k_2}, & I^* &= \frac{(pk_2 + (1-p)\sigma)\,\lambda^* S^*}{k_1 k_2}, \\ R^* &= \frac{\Big((1-p)\gamma_A k_1 + \gamma_I\,(pk_2 + (1-p)\sigma)\Big)\lambda^* S^*}{\mu k_1 k_2}. \end{aligned} \tag{11}$$

Substituting (11) in (10) gives,

$$\lambda^* S^* \left(1 + \frac{(pk_2 + (1-p)\sigma)}{k_1 k_2}\lambda^* + \frac{(1-p)}{k_2}\lambda^* \frac{((1-p)\gamma_A k_1 + \gamma_I\,(pk_2 + (1-p)\sigma))}{\mu k_1 k_2}\lambda^* - \frac{\beta_I(pk_2 + (1-p)\sigma)}{k_1 k_2} - \frac{\beta_A(1-p)}{k_2}\right) = 0. \tag{12}$$

Dividing (12) by $\lambda^* S^*$ ($\lambda^* S^* = 0$ corresponds to the disease-free equilibrium),

$$\begin{aligned} 1 + \frac{p(\mu+\gamma_I)k_2 + (1-p)((\mu+\gamma_I)\sigma + (\mu+\gamma_A)k_1)}{\mu k_1 k_2}\lambda^* &= \frac{p\beta_I k_2 + (1-p)(\beta_I\sigma + \beta_A k_1)}{k_1 k_2} \\ &= R_0. \end{aligned}$$

Therefore,

$$\lambda^* = \frac{\mu k_1 k_2 (R_0 - 1)}{p(\mu+\gamma_I)k_2 + (1-p)((\mu+\gamma_I)\sigma + (\mu+\gamma_A)k_1)} > 0, \qquad \text{when} \qquad R_0 > 1.$$

Substituting, λ^* in (9) gives endemic equilibrium $\mathcal{E}^*$:

$$
\begin{aligned}
S^* &= \frac{\Pi}{\mu}\left(\frac{pk_2(\mu+\gamma_I)+(1-p)(k_1k_2-\sigma\alpha)}{k_1k_2(R_0-1)+pk_2(\mu+\gamma_I)+(1-p)(k_1k_2-\sigma\alpha)}\right),\\
I^* &= \frac{\mu(pk_2+(1-p)\sigma)(R_0-1)S^*}{(\mu+\gamma_I)k_2p+(1-p)(k_1k_2-\sigma\alpha)},\\
A^* &= \frac{\mu k_1(1-p)(R_0-1)S^*}{(\mu+\gamma_I)k_2p+(1-p)(k_1k_2-\sigma\alpha)},\\
R^* &= \frac{(\gamma_I(pk_2+(1-p)\sigma)+\gamma_Ak_1(1-p))\,(R_0-1)S^*}{(\mu+\gamma_I)k_2p+(1-p)(k_1k_2-\sigma\alpha)}.
\end{aligned}
$$

The following lemma is demonstrated based on the above result.

Lemma 3.2. *If $R_0>1$, the Model (6) has a unique endemic equilibrium, denoted by $\mathcal{E}^*$.*

3.2.1 Local stability of $\mathcal{E}^*$

Following the method in [4], the local stability of endemic equilibrium is analyzed.

Theorem 3.2. *If $R_0>1$, then the endemic equilibrium $\mathcal{E}^*$ of the Model (6) is locally asymptotically stable (LAS).*

Proof. The local stability of $\mathcal{E}^*$ is analyzed by using center manifold theorem in [4]. For convenience, we denote $S=x_1$, $I=x_2$, $A=x_3$, $R=x_4$ and $N=x_1+x_2+x_3+x_4$. As a result, the model (6) can be rewritten as,

$$
\begin{aligned}
\frac{dx_1}{dt} &= \Pi-\frac{(\beta_Ix_2+\beta_Ax_3)x_1}{x_1+x_2+x_3+x_4}-\mu x_1,\\
\frac{dx_2}{dt} &= \frac{p(\beta_Ix_2+\beta_Ax_3)x_1}{x_1+x_2+x_3+x_4}+\sigma x_3-k_1x_2,\\
\frac{dx_3}{dt} &= \frac{(1-p)(\beta_Ix_2+\beta_Ax_3)x_1}{x_1+x_2+x_3+x_4}-k_2x_3,\\
\frac{dx_4}{dt} &= \gamma_Ix_2+\gamma_Ax_3-\mu x_4,
\end{aligned}
\tag{13}
$$

when $k_1=\mu+\gamma_I+\alpha$, $k_2=\mu+\gamma_A+\sigma$. Note that if $R_0=1$ then, $\beta_I=\beta^*=\dfrac{k_1(k_2-(1-p)\beta_A)}{pk_2+(1-p)\sigma}$. Jacobian of (13) at disease-free equilibrium point, $(x_1^*,x_2^*,x_3^*,x_4^*)=(\Pi/\mu,0,0,0)$ when $\beta_I=\beta^*$ is given by,

$$
J(\mathcal{E}_0)=\begin{bmatrix}
-\mu & -\beta^* & -\beta_A & 0\\
0 & p\beta^*-k_1 & p\beta_A+\sigma & 0\\
0 & (1-p)\beta^* & (1-p)\beta_A-k_2 & 0\\
0 & \gamma_I & \gamma_A & -\mu
\end{bmatrix}.
$$

Since $J(\mathcal{E}_0)$ has a simple eigenvalue 0 and other eigenvalues have negative real parts, the system (13) has a hyperbolic equilibrium point. The right eigenvector corresponding to the zero eigenvalue is expressed by $w=[w_1,w_2,w_3,w_4]^T$, where,

$$
w_1=-k_1k_2w_4,\qquad w_2=\mu(pk_2+(1-p)\sigma)w_4,\qquad w_3=(1-p)\mu k_1w_4,\qquad w_4=w_4>0.
$$

Further, the left eigenvector is denoted by $v = [v_1, v_2, v_3, v_4]$, where,

$$v_1 = 0, \quad v_2 = \beta^* v_3, \quad v_3 = v_3 > 0, \quad v_4 = 0.$$

Following, the expression of a and b in Theorem 4.1 [4], the associated non-zero partial derivatives of the system (13) are denoted by,

$$\frac{\partial^2 f_2}{\partial x_2^2} = -\frac{2p\mu\beta^*}{\Pi}, \qquad \frac{\partial^2 f_2}{\partial x_2 \partial x_3} = \frac{\partial^2 f_2}{\partial x_3 \partial x_2} = -\frac{p\mu(\beta^* + \beta_A)}{\Pi},$$
$$\frac{\partial^2 f_2}{\partial x_2 \partial x_4} = \frac{\partial^2 f_2}{\partial x_4 \partial x_2} = -\frac{p\mu\beta^*}{\Pi}, \qquad \frac{\partial^2 f_2}{\partial x_3^2} = -\frac{2p\mu\beta_A}{\Pi},$$
$$\frac{\partial^2 f_2}{\partial x_4 \partial x_3} = \frac{\partial^2 f_2}{\partial x_3 \partial x_4} = -\frac{p\mu\beta_A}{\Pi}, \qquad \frac{\partial^2 f_3}{\partial x_2^2} = -\frac{2(1-p)\mu\beta^*}{\Pi},$$
$$\frac{\partial^2 f_3}{\partial x_3 \partial x_2} = -\frac{(1-p)\mu(\beta^* + \beta_A)}{\Pi}, \qquad \frac{\partial^2 f_3}{\partial x_4 \partial x_2} = \frac{\partial^2 f_3}{\partial x_2 \partial x_4} = -\frac{(1-p)\mu\beta^*}{\Pi},$$
$$\frac{\partial^2 f_3}{\partial x_2 \partial x_3} = -\frac{(1-p)\mu(\beta^* + \beta_A)}{\Pi}, \qquad \frac{\partial^2 f_3}{\partial x_3^2} = -\frac{2(1-p)\mu\beta_A}{\Pi},$$
$$\frac{\partial^2 f_3}{\partial x_4 \partial x_3} = \frac{\partial^2 f_3}{\partial x_3 \partial x_4} = -\frac{(1-p)\mu\beta_A}{\Pi}, \qquad \frac{\partial^2 f_2}{\partial x_2 \partial \beta^*} = p, \qquad \frac{\partial^2 f_3}{\partial x_2 \partial \beta^*} = 1 - p.$$

Therefore,

$$\begin{aligned} a &= \sum_{i,j,k=1}^{4} v_k w_i w_j \frac{\partial^2 f_k}{\partial x_i \partial x_j}(0,0) \\ &= \sum_{i,j=1}^{4} v_2 w_i w_j \frac{\partial^2 f_2}{\partial x_i \partial x_j}(0,0) + \sum_{i,j=1}^{4} v_3 w_i w_j \frac{\partial^2 f_3}{\partial x_i \partial x_j}(0,0) \\ &= -\frac{2v_3 w_4^2 \mu^2 (1 - p + p\beta^*)(\mu(1-p)(k_1 + \sigma) + 1 + p\mu k_2)((1-p)(\beta_A k_1 + \beta^* \sigma) + p\beta^* k_2)}{\Pi} < 0, \end{aligned}$$

and

$$\begin{aligned} b &= \sum_{k,i=1}^{4} v_k w_i \frac{\partial^2 f_k}{\partial x_i \partial \beta^*}(0,0) \\ &= \sum_{i=1}^{4} v_2 w_i \frac{\partial^2 f_2}{\partial x_i \partial \beta^*}(0,0) + \sum_{i=1}^{4} v_3 w_i \frac{\partial^2 f_3}{\partial x_i \partial \beta^*}(0,0) \\ &= \mu v_3 w_4 ((1-p) + p\beta^*)((1-p)\sigma + pk_2) > 0. \end{aligned}$$

Consequently, $a < 0$ and $b > 0$ which correspond to Theorem 4.1(iv) in [4]. The endemic equilibrium $\mathcal{E}^*$ of Model (6), which is unique and exists when $R_0 > 1$, is locally asymptotically stable (LAS) whenever $R_0 > 1$ and $\beta_I > \beta^*$, with β_I being close to β^*. □

3.2.2 Global stability of endemic equilibrium

The global stability of $\mathcal{E}^*$ of the Model (6) for the case $\alpha = 0$ is focused in this section. The geometric approach for the global asymptotic stability of equilibria for nonlinear autonomous differential equations proposed in [20] based on the geometric criterion developed by Li and Muldowney [17, 18] is used to analyze the global stability of $\mathcal{E}^*$. Finally, the global stability of $\mathcal{E}^*$ is

demonstrated by using the following process in [28]. First, we show that system (6) is uniformly persistence.

Definition 3.1. *System (6) is said to be uniformly persistence if there exist a constant $0 < \varepsilon_0 < \Pi/\mu$ such that any solution $x(t) = (S(t), I(t), A(t), R(t))$ with $x(0) \in \mathring{\Omega}$ satisfies,*

$$\min\left\{\lim_{t\to\infty}\inf S(t), \lim_{t\to\infty}\inf I(t), \lim_{t\to\infty}\inf A(t), \lim_{t\to\infty}\inf R(t)\right\} \geq \varepsilon_0. \tag{14}$$

The uniformly persistence of the model (6) is shown by using Theorem 4.3 in [9]. In order to satisfy the requirements of the theory, we choose $X = \mathbb{R}^4$,$E = \Omega$ and N is the largest invariant set on the boundary $\partial\Omega$ which consist of a singleton $\mathcal{E}_0$ and is isolated. Combining with the Lemma 3.1, $\mathcal{E}_0$ is unstable when $R_0 > 1$ and following theorem is established.

Theorem 3.3. *System (6) is uniformly persistent in $\mathring{\Omega}$ if and only if $R_0 > 1$.*

In order to provide global stability, it is essential that the system of equations fulfills all four assumptions described in [20]. We start with the set of invariant manifolds in a system of autonomous differential equations. Let $f(x)$ be a continuous function that can find derivatives on domain D and range of $f(x)$ is the set of $\mathbb{R}^n$. The system of autonomous differential equations is written in the form:

$$x' = f(x), \qquad x \in D \subset \mathbb{R}^n, \tag{15}$$

where $x(t, x_0)$ is the solution of the system (15) that satisfies the initial condition $x(0, x_0) = x_0$. From Proposition 3.1 in [18], let $g(x)$ be an $\mathbb{R}^m-$valued function in $\mathbb{R}^n$ with $\dim\left(\dfrac{\partial g}{\partial x}\right) = m$ if $g(x) = 0$. The set

$$\Omega = \{x \in \mathbb{R}^n | g(x) = 0\},$$

is an invariant manifold of the system (15) if and only if,

$$g_f(x) = \frac{\partial g}{\partial x} \cdot f(x) = N(x) \cdot g(x),$$

where $N(x)$ is a continuous matrix-valued function with size $m \times m$. $g_f(x)$ is a matrix in which each element is replaced with a derivative with respect to f. Further, $v(x)$ is a real-valued function on Ω, where $v(x) = tr(N(x))$. The first three assumptions for proving global stability are:

- **(H1)** Ω is simply connected.
- **(H2)** There is a compact absorbing set $K \subset D \subset \Omega$.
- **(H3)** x^* is the unique equilibrium of system (15) in $D \subset \Omega$ which satisfies $f(x^*) = 0$.

Next is the process for final assumptions, starting with considering the linear differential equation that corresponds to (15), which is written in the form:

$$z'(t) = \left[P_f P^{-1} + P\frac{\partial f^{[m+2]}}{\partial x}P^{-1} - v(x)I\right] z(t) =: B(x(t, x_0))z(t), \tag{16}$$

where $P(x)$ is a C^1 nonsingular $\binom{n}{m+2} \times \binom{n}{m+2}$ matrix-valued function in Ω in which $||P^{-1}(x)||$ is uniformly bounded for $x \in K$ and P_f is a matrix in which each element is replaced with a derivative with respect to f, and $J^{[m+2]}$ is the $m + 2$ additive compound matrix of the Jacobian matrix of (15). The fourth assumption is derived from the matrix $B(x(t, x_0))$ in (16) as expressed in the following:

(H4) Let $b_{ij}(t)$ and $c_{ij}(t)$ are each elements of matrix $B(x(t,x_0))$ and $C(t)$, respectively.

There exist number $\alpha_i > 0, i = 1 \dots n$ such that for all $t > T_1 > 0$ and all $x_0 \in K$ it holds,

$$b_{ii}(t) + \Sigma_{i\neq j}\frac{\alpha_j}{\alpha_i}|b_{ij}(t)| \leq c_{ii}(t) + \Sigma_{i\neq j}\frac{\alpha_j}{\alpha_i}|c_{ij}(t)|,$$

and

$$\lim_{t\to\infty}\frac{1}{t}\int_0^t c_{ii}(s) + \Sigma_{i\neq j}\frac{\alpha_j}{\alpha_i}|c_{ij}(s)|ds = h_i < 0.$$

From Theorem 13 in [28], if assumptions (**H1**)−(**H4**) are satisfied, the following lemma is established.

Lemma 3.3. *The unique endemic equilibrium x^* of (15) is globally asymptotically stable in $D \subset \Omega$.*

The global stability of $\mathcal{E}^*$ is proved by using Theorem 3.3 and Lemma 3.3 as shown in following:

Theorem 3.4. *If $\alpha = 0$, then endemic equilibrium $\mathcal{E}^*$ of the system (6) is globally asymptotically stable when $R_0 > 1$ and conditions,*

$$\begin{aligned}
3(k_1+k_2) &> p\beta_I + (1-p)\beta_A,\\
(1-p)\beta_A &< k_1,\\
p\varepsilon(\beta_A+\beta_I) + k_1 &> 2p\beta_I,\\
k_2 + \varepsilon(\beta_A+\beta_I) &> p\beta_I,\\
k_1 + k_2 + \varepsilon(\beta_A+\beta_I) &> p\beta_I + (1-p)\beta_A,\\
\frac{\sigma(1-p)k_1}{pk_2}\left(\frac{(1-p)k_1\gamma_A}{pk_2\gamma_I}+1\right) &< \mu,
\end{aligned}$$

are satisfied.

Proof. First, we define $g(X) = S + I + A + R - \Pi/\mu$ where $X = (S, I, A, R) \in \mathbb{R}^4_+$, the invariant manifold of the system (6) is

$$\Omega = \left\{X \in \mathcal{R}^4_+ | g(X) = 0\right\}.$$

By Li and Muldowney in [18], $N(x) = v(x) = -\mu$ and $m = \dim\left(\frac{\partial g}{\partial X}\right) = 1$. It is evident that (**H1**) is true. Furthermore, for $R_0 > 1$, (**H2**)-(**H3**) can be deduced from Theorem 3.3 and Lemma 3.2.

From (14), there exists $T > 0$ such that for $t > T$,

$$\varepsilon_0 < S(t), I(t), A(t), R(t) \leq \frac{\Pi}{\mu}. \tag{17}$$

For convenience, let $\frac{S}{N} = s$, $\frac{I}{N} = i$, $\frac{A}{N} = a$ and $\frac{R}{N} = r$. Thus, (17) is rewritten as,

$$\varepsilon \leq s, i, a, r \leq 1, \quad \text{and} \quad s + i + a + r = 1, \tag{18}$$

when $\varepsilon = \varepsilon_0\mu/\Pi$. The Jacobian matrix of (6) may be expressed as,

$$J = -\mu I_{4\times 4} + \Phi,$$

where $I_{4\times4}$ is the 4×4 identity matrix and

$$\Phi = \begin{bmatrix} -\lambda(1-s) & (\lambda-\beta_I)s & (\lambda-\beta_A)s & \lambda s \\ p\lambda(1-s) & ps(\beta_I-\lambda)-(\gamma_I+\alpha) & ps(\beta_A-\lambda)+\sigma & -p\lambda s \\ (1-p)\lambda(1-s) & (1-p)s(\beta_I-\lambda) & (1-p)s(\beta_A-\lambda)-(\gamma_A+\sigma) & -(1-p)\lambda s \\ 0 & \gamma_I & \gamma_A & 0 \end{bmatrix},$$

where $\lambda = \beta_I i + \beta_A a$. According to the definition of the third additive compound matrix in [18], we get

$$J^{[3]} = \Phi^{[3]} - 3\mu I_{4\times4},$$

with

$$\Phi^{[3]} = \left(\phi_1^{[3]}, \phi_2^{[3]}, \phi_3^{[3]}, \phi_4^{[4]}\right)^T,$$

where

$$\phi_1^{[3]} = \begin{bmatrix} -\lambda(1-s)+(p\beta_I+(1-p)\beta_A-\lambda)s-(\gamma_A+\gamma_I+\sigma+\alpha) \\ -(1-p)\lambda s \\ p\lambda s \\ \lambda s \end{bmatrix},$$

$$\phi_2^{[3]} = \begin{bmatrix} \gamma_A \\ -\lambda(1-s)+p\beta_I s(1-i)-p\beta_A sa-(\gamma_I+\alpha) \\ p\beta_A s-p\lambda s+\sigma \\ \beta_A s-\lambda s \end{bmatrix},$$

$$\phi_3^{[3]} = \begin{bmatrix} -\gamma_I \\ (1-p)\beta_I s-(1-p)\lambda s \\ -\lambda(1-s)+(1-p)\beta_A s-(1-p)\lambda s-(\gamma_A+\sigma) \\ \lambda s-\beta_I s \end{bmatrix},$$

$$\phi_4^{[3]} = \begin{bmatrix} 0 \\ -(1-p)\lambda(1-s) \\ p\lambda(1-s) \\ (p\beta_I+(1-p)\beta_A)s-(\gamma_A+\gamma_I+\sigma+\alpha) \end{bmatrix}.$$

Let $P(x)$ be a diagonal matrix such that,

$$P(x) = \text{diag}\left\{r, a, i, s\right\},$$

follows direct computational from (16), this yield,

$$B(t) = P_f P^{-1} + PJ^{[3]}P^{-1} + \mu I_{4\times4} = \text{diag}\left\{\frac{r'}{r}, \frac{a'}{a}, \frac{i'}{i}, \frac{s'}{s}\right\} + P\Phi^{[3]}P^{-1} - 2\mu I_{4\times4},$$

where

$$P\Phi^{[3]}P^{-1} = \left(\zeta_1^{[3]}, \zeta_2^{[3]}, \zeta_3^{[3]}, \zeta_4^{[3]}\right)^T,$$

$$\zeta_1^{[3]} = \begin{bmatrix} -\lambda(1-s) + (p\beta_I + (1-p)\beta_A - \lambda)s - (\gamma_I + \gamma_A + \sigma + \alpha) \\ -(1-p)\lambda\frac{sr}{a} \\ p\lambda\frac{sr}{i} \\ \lambda r \end{bmatrix},$$

$$\zeta_2^{[3]} = \begin{bmatrix} \gamma_A\frac{a}{r} \\ -\lambda(1-s) + p\beta_I s(1-i) - p\beta_A sa - (\gamma_I + \alpha) \\ p\beta_A\frac{sa}{i} - p\lambda\frac{sa}{i} + \sigma\frac{a}{i} \\ \beta_A a - \lambda a \end{bmatrix},$$

$$\zeta_3^{[3]} = \begin{bmatrix} -\gamma_I\frac{i}{r} \\ (1-p)\beta_I\frac{si}{a} - (1-p)\lambda\frac{si}{a} \\ -\lambda(1-s) + (1-p)\beta_A s - (1-p)\lambda s - (\gamma_A + \sigma) \\ \lambda i - \beta_I i \end{bmatrix},$$

$$\zeta_4^{[3]} = \begin{bmatrix} 0 \\ -(1-p)\lambda(1-s)\frac{s}{a} \\ p\lambda(1-s)\frac{s}{i} \\ (p\beta_I + (1-p)\beta_A - \lambda)s - (\gamma_A + \gamma_I + \sigma + \alpha) \end{bmatrix}.$$

Observe that (6) can be rewritten as,

$$\frac{S'}{S} = \frac{\Pi}{\mu} - \beta_I i - \beta_A a - \mu, \tag{19}$$

$$p\beta_A\frac{sa}{i} = \frac{I'}{I} - p\beta_I s + k_1, \tag{20}$$

$$(1-p)\beta_I\frac{si}{a} = \frac{A'}{A} - (1-p)\beta_A s + k_2, \tag{21}$$

$$\frac{R'}{R} = \gamma_I\frac{i}{r} + \gamma_A\frac{a}{r} - \mu, \tag{22}$$

$$\frac{a}{i} = \frac{(1-p)k_1}{pk_2} + \frac{(1-p)}{pk_2}\frac{I'}{I} - \frac{1}{k_2}\frac{A'}{I}. \tag{23}$$

For convenience in proof, the next process is considered by separating in two cases.

Case I: In the case $\beta_A - \lambda > 0$. By (18) and (19)−(23), it can be reveal that,

$$\begin{aligned} h_1(t) &= b_{11}(t) + \Sigma_{j=2}^4 |b_{1j}(t)| \\ &= -\lambda(1-s) + (p\beta_I + (1-p)\beta_A - \lambda)s - (k_1 + k_2) + (1-p)\lambda\frac{sr}{a} + p\lambda\frac{sr}{i} + \lambda r + \frac{r'}{r} \\ &= -\lambda(1-s) + (p\beta_I + (1-p)\beta_A - \lambda)s - (k_1 + k_2) \\ &\quad + \left((1-p)\beta_A s + p\beta_I s + (1-p)\beta_I\frac{si}{a} + p\beta_A\frac{sa}{i}\right)r + \lambda r + \frac{r'}{r} \\ &= -\lambda(1-s) + (p\beta_I + (1-p)\beta_A - \lambda)s - (k_1 + k_2) + \Bigg((1-p)\beta_A s + p\beta_I s \\ &\quad + \left(\frac{A'}{A} - (1-p)\beta_A s + k_2\right) + \left(\frac{I'}{I} - p\beta_I s + k_1\right)\Bigg)r + \lambda r + \frac{r'}{r} \end{aligned}$$

$$
\begin{aligned}
&= -\lambda(1-r) + (p\beta_I + (1-p)\beta_A)s - (k_1+k_2)(1-r) + \frac{r'}{r} + \frac{A'}{A}r + \frac{I'}{I}r \\
&= -\lambda(1-r) - \Big(k_1+k_2 - (p\beta_I + (1-p)\beta_A)\Big)s - (k_1+k_2)(i+a) + \frac{r'}{r} \\
&\quad + \frac{A'}{A}r + \frac{I'}{I}r \\
&\leq -3\varepsilon^2(\beta_I+\beta_A) - \varepsilon\Big(k_1+k_2 - (p\beta_I + (1-p)\beta_A)\Big) - 2\varepsilon(k_1+k_2) + \frac{r'}{r} \\
&\quad + \frac{A'}{A}r + \frac{I'}{I}r \\
&\leq -\varepsilon\Big(3(k_1+k_2) - (p\beta_I + (1-p)\beta_A)\Big) + \frac{r'}{r} + \frac{A'}{A} + \frac{I'}{I} \cong \hat{h}_1(t).
\end{aligned}
$$

$$
\begin{aligned}
h_2(t) &= b_{22}(t) + \Sigma_{j\neq 2}|b_{2j}(t)| \\
&= -\lambda(1-s) + p\beta_I s(1-i) - p\beta_A sa - (k_1+\mu) + \gamma_A\frac{a}{r} \\
&\quad + (\beta_A-\lambda)p\frac{sa}{i} + \sigma\frac{a}{i} + (\beta_A-\lambda)a + \frac{a'}{a} \\
&= -(\beta_I i + \beta_A a)(1-s) + p\beta_I s(1-i) - p\beta_A sa - (k_1+\mu) + \Big(\mu - \gamma_I\frac{i}{r} + \frac{R'}{R}\Big) \\
&\quad + \left(p\beta_A\frac{(1-a)sa}{i} - p\beta_I sa\right) + \sigma\left(\frac{(1-p)k_1}{pk_2} + \frac{(1-p)}{pk_2}\frac{I'}{I} - \frac{A'}{k_2 I}\right) \\
&\quad + \left(a\beta_A(1-a) - \beta_I ai\right) + \frac{a'}{a} \\
&= -\beta_A a - \beta_I i(1-s) + p\beta_I s(1-i) + (1-p)\beta_A sa - k_1 - \gamma_I\frac{i}{r} \\
&\quad + (1-a)\left(\frac{I'}{I} - p\beta_I s + k_1\right) - p\beta_I sa + \frac{\sigma(1-p)k_1}{pk_2} \\
&\quad + \left(\beta_A(1-a)a - \beta_I ai\right) + \frac{a'}{a} + \frac{R'}{R} + \frac{\sigma(1-p)}{pk_2}\frac{I'}{I} - \sigma\frac{A'}{k_2 I} \\
&= -\beta_I i(1-s) - p\beta_I si + (1-p)\beta_A sa - \gamma_I\frac{i}{r} - k_1 a + \frac{\sigma(1-p)k_1}{pk_2} \\
&\quad - \beta_A a^2 - \beta_I ai + \frac{a'}{a} + \frac{R'}{R} + \frac{\sigma(1-p)}{pk_2}\frac{I'}{I} - \sigma\frac{A'}{k_2 I} + (1-a)\frac{I'}{I} \\
&= \left(\frac{\sigma(1-p)k_1}{pk_2} - \beta_I i(1-s) - p\beta_I si - \gamma_I\frac{i}{r}\right) + a\Big((1-p)\beta_A s - k_1 - \beta_A a - \beta_I i\Big) \\
&\quad + \frac{a'}{a} + \frac{R'}{R} + \frac{\sigma(1-p)}{pk_2}\frac{I'}{I} - \sigma\frac{A'}{k_2 I} + (1-a)\frac{I'}{I} \\
&\leq \left(\frac{\sigma(1-p)k_1}{pk_2} - \gamma_I\frac{i}{r}\right) - a\Big(k_1 - (1-p)\beta_A\Big) + \frac{a'}{a} + \frac{R'}{R} + \frac{\sigma(1-p)}{pk_2}\frac{I'}{I} - \sigma\frac{A'}{I} \\
&\quad + (1-a)\frac{I'}{I}.
\end{aligned}
$$

The conditions of $h_2(t)$ are separate in two cases:

Case I.I) By assumption $\gamma_I \frac{i}{r} > \frac{\sigma(1-p)k_1}{pk_2}$, then,

$$\begin{aligned} h_2(t) &\leq \left(\frac{\sigma(1-p)k_1}{pk_2} - \gamma_I\frac{i}{r}\right) - a\Big(k_1 - (1-p)\beta_A\Big) + \frac{a'}{a} + \frac{R'}{R} + \frac{\sigma(1-p)}{pk_2}\frac{I'}{I} \\ &\quad - \sigma\frac{A'}{k_2 I} + (1-a)\frac{I'}{I} \\ &\leq -a\Big(k_1 - (1-p)\beta_A\Big) + \frac{a'}{a} + \frac{R'}{R} + \frac{\sigma(1-p)}{pk_2}\frac{I'}{I} + (1-a)\frac{I'}{I} \\ &\leq -\varepsilon\Big(k_1 - (1-p)\beta_A\Big) + \frac{a'}{a} + \frac{R'}{R} + \frac{\sigma(1-p)}{pk_2}\frac{I'}{I} + (1-a)\frac{I'}{I} \cong \hat{h}_{2a}(t). \end{aligned}$$

Case I.II) By assumption $\gamma_I \frac{i}{r} < \frac{\sigma(1-p)k_1}{pk_2}$.

For this case,

$$\begin{aligned} \gamma_A\frac{a}{r} &< \gamma_A\frac{\sigma(1-p)k_1}{pk_2\gamma_I}\frac{a}{i} \\ &= \frac{\gamma_A\sigma(1-p)k_1}{pk_2\gamma_I}\left(\frac{(1-p)k_1}{pk_2} + \frac{(1-p)}{pk_2}\frac{I'}{I} - \frac{1}{k_2}\frac{A'}{I}\right). \end{aligned}$$

Thus,

$$\begin{aligned} h_2(t) &= -\lambda(1-s) + p\beta_I s(1-i) - p\beta_A sa - (k_1+\mu) + \gamma_A\frac{a}{r} \\ &\quad + (\beta_A - \lambda)p\frac{sa}{i} + \sigma\frac{a}{i} + (\beta_A - \lambda)a + \frac{a'}{a} \\ &\leq -(\beta_I i + \beta_A a)(1-s) + p\beta_I s(1-i) - p\beta_A sa - (k_1+\mu) \\ &\quad + \frac{\gamma_A\sigma(1-p)k_1}{pk_2\gamma_I}\left(\frac{(1-p)k_1}{pk_2} + \frac{(1-p)}{pk_2}\frac{I'}{I} - \frac{1}{k_2}\frac{A'}{I}\right) \\ &\quad + \left(p\beta_A\frac{(1-a)sa}{i} - p\beta_I sa\right) + \sigma\left(\frac{(1-p)k_1}{pk_2} + \frac{(1-p)}{pk_2}\frac{I'}{I} - \frac{A'}{k_2 I}\right) \\ &\quad + \left(a\beta_A(1-a) - \beta_I ai\right) + \frac{a'}{a} \\ &= -\beta_I i(1-s) + p\beta_I s(1-i) + (1-p)\beta_A sa - (k_1+\mu) \\ &\quad + \frac{\gamma_A\sigma(1-p)k_1}{pk_2\gamma_I}\left(\frac{(1-p)k_1}{pk_2} + \frac{(1-p)}{pk_2}\frac{I'}{I} - \frac{1}{k_2}\frac{A'}{I}\right) \\ &\quad + (1-a)\left(\frac{I'}{I} - p\beta_I s + k_1\right) + \sigma\left(\frac{(1-p)k_1}{pk_2} + \frac{(1-p)}{pk_2}\frac{I'}{I} - \frac{A'}{k_2 I}\right) \\ &\quad - p\beta_I sa - \beta_A a^2 - \beta_I ai + \frac{a'}{a}, \\ &\leq -\beta_I i(1-s) - p\beta_I si + a\left((1-p)\beta_A s - k_1\right) - \mu \\ &\quad + \frac{\sigma(1-p)k_1}{pk_2}\left(\frac{(1-p)k_1\gamma_A}{pk_2\gamma_I} + 1\right) + \frac{a'}{a} + (1-a)\frac{I'}{I} \\ &\quad + \frac{\sigma(1-p)}{pk_2}\frac{I'}{I} + \frac{\gamma_A\sigma(1-p)k_1}{pk_2\gamma_I}\left(\frac{(1-p)}{pk_2}\right)\frac{I'}{I} \end{aligned}$$

$$\leq -\varepsilon\Big(k_1-(1-p)\beta_A s\Big)-\left(\mu-\frac{\sigma(1-p)k_1}{pk_2}\left(\frac{(1-p)k_1\gamma_A}{pk_2\gamma_I}+1\right)\right)$$
$$+\frac{a'}{a}+(1-a)\frac{I'}{I}+\frac{\sigma(1-p)}{pk_2}\frac{I'}{I}+\frac{\gamma_A\sigma(1-p)k_1}{pk_2\gamma_I}\left(\frac{(1-p)}{pk_2}\right)\frac{I'}{I}\cong \hat{h}_{2b}(t).$$

$$h_3(t)=b_{33}(t)+\Sigma_{j\neq 3}|b_{3j}(t)|$$
$$=-\lambda(1-s)+(1-p)\beta_A s-(1-p)\lambda s-\gamma_A-\sigma-2\mu+\gamma_I\frac{i}{r}$$
$$+(1-p)(\beta_I-\lambda)\frac{si}{a}+(\beta_I-\lambda)i+\frac{i'}{i}$$
$$=-\lambda(1-s)+(1-p)(1-a)\beta_A s-(1-p)\beta_I si-\gamma_A-\sigma-2\mu$$
$$+\left(\frac{R'}{R}-\gamma_A\frac{a}{r}+\mu\right)+(1-p)\beta_I\frac{si}{a}(1-i)-(1-p)\beta_A si+\beta_I(1-i)i$$
$$-\beta_A ai+\frac{i'}{i}$$
$$=-\beta_I i(1-s)-\beta_A a(1-s)+(1-p)(1-a)\beta_A s-(1-p)\beta_I si-k_2-\gamma_A\frac{a}{r}$$
$$+\left(\frac{A'}{A}-(1-p)\beta_A s+k_2\right)(1-i)-(1-p)\beta_A si+\beta_I(1-i)i-\beta_A ai$$
$$+\frac{i'}{i}+\frac{R'}{R}$$
$$=i\Big(\beta_I(1-i)-\beta_I(1-s)-(1-p)\beta_I s-k_2-\beta_A a\Big)-\beta_A a(1-s)$$
$$-(1-p)\beta_A sa-\gamma_A\frac{a}{r}+\frac{i'}{i}+\frac{R'}{R}+(1-i)\frac{A'}{A}$$
$$=i\Big(\beta_I(1-i)-\beta_I(1-s)-(1-p)\beta_I s-k_2-\beta_A a\Big)-\beta_A a(1-s)$$
$$-(1-p)\beta_A sa-\gamma_A\frac{a}{r}+\frac{i'}{i}+\frac{R'}{R}+(1-i)\frac{A'}{A}$$
$$=-i\Big(k_2+\beta_A a+\beta_I i-p\beta_I s\Big)-\beta_A a(1-s)-(1-p)\beta_A sa-\gamma_A\frac{a}{r}+\frac{i'}{i}$$
$$+\frac{R'}{R}+(1-i)\frac{A'}{A}$$
$$\leq -\varepsilon\Big(k_2+\varepsilon(\beta_A+\beta_I)-p\beta_I\Big)+\frac{i'}{i}+\frac{R'}{R}+(1-i)\frac{A'}{A}\cong \hat{h}_3(t).$$

$$h_4(t)=b_{44}(t)+\Sigma_{j=1}^{3}|b_{4j}(t)|$$
$$=\big(p\beta_I+(1-p)\beta_A-\lambda\big)s-(\gamma_A+\gamma_I+\sigma+\alpha)+(1-p)\lambda(1-s)\frac{s}{a}$$
$$+p\lambda(1-s)\frac{s}{i}-2\mu+\frac{s'}{s}$$
$$=\big(p\beta_I+(1-p)\beta_A-\lambda\big)s-k_1-k_2+(1-p)\beta_I\frac{si}{a}(1-s)+(1-p)\beta_A s(1-s)$$
$$+p\beta_I s(1-s)+p\beta_A\frac{sa}{i}(1-s)+\frac{s'}{s}$$
$$=\big(p\beta_I+(1-p)\beta_A-\lambda\big)s-k_1-k_2+\left(\frac{A'}{A}-(1-p)\beta_A s+k_2\right)(1-s)$$
$$+(1-p)\beta_A s(1-s)+p\beta_I s(1-s)+\left(\frac{I'}{I}-p\beta_I s+k_1\right)(1-s)+\frac{s'}{s}$$

$$
\begin{aligned}
&= -s\big(k_1 + k_2 + \beta_I i + \beta_A a - p\beta_I - (1-p)\beta_A\big) + \frac{s'}{s} + (1-s)\frac{A'}{A} + (1-s)\frac{I'}{I} \\
&\leq -\varepsilon\big(k_1 + k_2 + \varepsilon(\beta_I + \beta_A) - p\beta_I - (1-p)\beta_A\big) + \frac{s'}{s} + (1-\varepsilon)\frac{A'}{A} + (1-\varepsilon)\frac{I'}{I} \\
&\cong \hat{h}_4(t).
\end{aligned}
$$

By the conditions,

$$
\begin{aligned}
3(k_1 + k_2) &> p\beta_I + (1-p)\beta_A, \\
k_1 &> (1-p)\beta_A, \\
k_2 + \varepsilon(\beta_A + \beta_I) &> p\beta_I, \\
k_1 + k_2 + \varepsilon(\beta_A + \beta_I) &> p\beta_I + (1-p)\beta_A, \\
\mu &> \frac{\sigma(1-p)k_1}{pk_2}\left(\frac{(1-p)k_1\gamma_A}{pk_2\gamma_I} + 1\right),
\end{aligned}
$$

and based on (18). Taking the matrix $C_1(t) = \text{diag}\Big\{\hat{h}_1(t), \hat{h}_{2a}(t), \hat{h}_3(t), \hat{h}_4(t)\Big\}$ and $C_2(t) = \text{diag}\Big\{\hat{h}_1(t), \hat{h}_{2b}(t), \hat{h}_3(t), \hat{h}_4(t)\Big\}$ in **(H4)** results in,

$$
\lim_{t\to\infty} \frac{1}{t}\int_0^t \hat{h}_i(s)ds = \hat{H}_i < 0, \qquad i = 1, 2a, 2b, 3, 4,
$$

where

$$
\begin{aligned}
\hat{H}_1 &= -\varepsilon\big(3(k_1 + k_2) - (p\beta_I + (1-p)\beta_A)\big), \\
\hat{H}_{2a} &= -\varepsilon\big(k_1 - (1-p)\beta_A\big), \\
\hat{H}_{2b} &= -\varepsilon\Big(k_1 - (1-p)\beta_A s\Big) - \left(\mu - \frac{\sigma(1-p)k_1}{pk_2}\left(\frac{(1-p)k_1\gamma_A}{pk_2\gamma_I} + 1\right)\right), \\
\hat{H}_3 &= -\varepsilon\big(k_2 + \varepsilon(\beta_A + \beta_I) - p\beta_I\big),
\end{aligned}
$$

and

$$
\hat{H}_4 = -\varepsilon\big(k_1 + k_2 + \varepsilon(\beta_A + \beta_I) - p\beta_I - (1-p)\beta_A\big).
$$

Case II: In the case $\beta_A - \lambda < 0$. Using similar arguments in **Case I** yields,

$$
\begin{aligned}
h_1(t) &= -\lambda(1-s) + (p\beta_I + (1-p)\beta_A - \lambda)s - (k_1 + k_2) + (1-p)\lambda\frac{sr}{a} + p\lambda\frac{sr}{i} + \lambda r + \frac{r'}{r} \\
&= -\lambda(1-r) - \Big(k_1 + k_2 - (p\beta_I + (1-p)\beta_A)\Big)s - (k_1 + k_2)(i + a) + \frac{r'}{r} + \frac{A'}{A}r + \frac{I'}{I}r \\
&\leq -3\varepsilon^2(\beta_I + \beta_A) - \varepsilon\Big(k_1 + k_2 - (p\beta_I + (1-p)\beta_A)\Big) - 2\varepsilon(k_1 + k_2) + \frac{r'}{r} + \frac{A'}{A}r + \frac{I'}{I}r \\
&\leq -\varepsilon\Big(3(k_1 + k_2) - (p\beta_I + (1-p)\beta_A)\Big) + \frac{r'}{r} + \frac{A'}{A} + \frac{I'}{I} \cong \bar{h}_1(t).
\end{aligned}
$$

$$
\begin{aligned}
h_2(t) &= -\lambda(1-s) + p\beta_I s(1-i) - p\beta_A sa - (k_1+\mu) + \gamma_A \frac{a}{r} \\
&\quad + (\lambda-\beta_A)p\frac{sa}{i} + \sigma\frac{a}{i} + (\lambda-\beta_A)a + \frac{a'}{a} \\
&= -\lambda(i+a+r) + p\beta_I s(1-i) - p\beta_A sa - (k_1+\mu) \\
&\quad + \left(\frac{R'}{R} + \mu - \gamma_I\frac{i}{r}\right) + p\beta_I sa - p\beta_A\frac{sa}{i}(1-a) + \frac{\sigma(1-p)k_1}{pk_2} \\
&\quad + \frac{\sigma(1-p)}{pk_2}\frac{I'}{I} - \sigma\frac{A'}{k_2 I} + \lambda a - \beta_A a + \frac{a'}{a} \\
&= -\lambda(i+r) + p\beta_I s(1-i) - p\beta_A sa - k_1 + \frac{R'}{R} - \gamma_I\frac{i}{r} \\
&\quad + p\beta_I sa - \left(\frac{I'}{I} - p\beta_I s + k_1\right)(1-a) + \frac{\sigma(1-p)k_1}{pk_2} + \frac{\sigma(1-p)}{pk_2}\frac{I'}{I} \\
&\quad - \sigma\frac{A'}{k_2 I} - \beta_A a + \frac{a'}{a} \\
&= -\lambda(i+r) + 2p\beta_I s - p\beta_I si - p\beta_A sa - k_1 - k_1(s+i+r) + \frac{R'}{R} - \gamma_I\frac{i}{r} \\
&\quad - \frac{I'}{I}(1-a) + \frac{\sigma(1-p)k_1}{pk_2} + \frac{\sigma(1-p)}{pk_2}\frac{I'}{I} - \sigma\frac{A'}{I} - \beta_A a + \frac{a'}{a} \\
&\leq -s(p\beta_I i + p\beta_A a + k_1 - 2p\beta_I) + \frac{R'}{R} + \frac{\sigma(1-p)k_1}{pk_2} + \frac{\sigma(1-p)}{pk_2}\frac{I'}{I} + \frac{a'}{a} \\
&\leq -\varepsilon(p\varepsilon(\beta_I+\beta_A) + k_1 - 2p\beta_I) + \frac{R'}{R} + \frac{\sigma(1-p)k_1}{pk_2} + \frac{\sigma(1-p)}{pk_2}\frac{I'}{I} + \frac{a'}{a} \cong \bar{h}_2(t).
\end{aligned}
$$

$$
\begin{aligned}
h_3(t) &= b_{33}(t) + \Sigma_{j\neq 3}|b_{3j}(t)| \\
&= -\lambda(1-s) + (1-p)\beta_A s - (1-p)\lambda s - \gamma_A - \sigma - 2\mu + \gamma_I\frac{i}{r} \\
&\quad + (1-p)(\beta_I-\lambda)\frac{si}{a} + (\beta_I-\lambda)i + \frac{i'}{i} \\
&= -\lambda(1-s) + (1-p)(1-a)\beta_A s - (1-p)\beta_I si - \gamma_A - \sigma - 2\mu \\
&\quad + \left(\frac{R'}{R} - \gamma_A\frac{a}{r} + \mu\right) + (1-p)\beta_I\frac{si}{a}(1-i) - (1-p)\beta_A si + \beta_I(1-i)i - \beta_A ai + \frac{i'}{i} \\
&= -\beta_I i(1-s) - \beta_A a(1-s) + (1-p)(1-a)\beta_A s - (1-p)\beta_I si - k_2 - \gamma_A\frac{a}{r} \\
&\quad + \left(\frac{A'}{A} - (1-p)\beta_A s + k_2\right)(1-i) - (1-p)\beta_A si + \beta_I(1-i)i - \beta_A ai + \frac{i'}{i} + \frac{R'}{R} \\
&= -i\Big(k_2 + \beta_A a + \beta_I i - p\beta_I s\Big) - \beta_A a(1-s) - (1-p)\beta_A sa - \gamma_A\frac{a}{r} + \frac{i'}{i} + \frac{R'}{R} \\
&\quad + (1-i)\frac{A'}{A} \\
&\leq -\varepsilon\Big(k_2 + \varepsilon(\beta_A+\beta_I) - p\beta_I\Big) + \frac{i'}{i} + \frac{R'}{R} + (1-i)\frac{A'}{A} \cong \bar{h}_3(t).
\end{aligned}
$$

$$
\begin{aligned}
h_4(t) &= b_{44}(t) + \Sigma_{j=1}^{3}|b_{4j}(t)| \\
&= \big(p\beta_I + (1-p)\beta_A - \lambda\big)s - (\gamma_A + \gamma_I + \sigma + \alpha) + (1-p)\lambda(1-s)\frac{s}{a} \\
&\quad + p\lambda(1-s)\frac{s}{i} - 2\mu + \frac{s'}{s} \\
&= \big(p\beta_I + (1-p)\beta_A - \lambda\big)s - k_1 - k_2 + \left(\frac{A'}{A} - (1-p)\beta_A s + k_2\right)(1-s) \\
&\quad + (1-p)\beta_A s(1-s) + p\beta_I s(1-s) + \left(\frac{I'}{I} - p\beta_I s + k_1\right)(1-s) + \frac{s'}{s} \\
&= -s\big(k_1 + k_2 + \beta_I i + \beta_A a - p\beta_I - (1-p)\beta_A\big) + \frac{s'}{s} + (1-s)\frac{A'}{A} + (1-s)\frac{I'}{I} \\
&\leq -\varepsilon\big(k_1 + k_2 + \varepsilon(\beta_I + \beta_A) - p\beta_I - (1-p)\beta_A\big) + \frac{s'}{s} + (1-\varepsilon)\frac{A'}{A} + (1-\varepsilon)\frac{I'}{I} \\
&\cong \bar{h}_4(t).
\end{aligned}
$$

Then, the matrix $C(t)$ in condition **(H4)** as,

$$C(t) = \text{diag}\big(\bar{h}_1(t), \bar{h}_2(t), \bar{h}_3(t), \bar{h}_4(t)\big),$$

based on (18) and conditions,

$$
\begin{aligned}
3(k_1 + k_2) &> p\beta_I + (1-p)\beta_A, \\
p\varepsilon(\beta_A + \beta_I) + k_1 &> 2p\beta_I, \\
k_2 + \varepsilon(\beta_A + \beta_I) &> p\beta_I, \\
k_1 + k_2 + \varepsilon(\beta_A + \beta_I) &> p\beta_I + (1-p)\beta_A,
\end{aligned}
$$

it shown that,

$$\lim_{t\to+\infty} \frac{1}{t}\int_0^t \bar{h}_i(s)ds = \bar{H}_i < 0, \qquad i = 1, \ldots, 4,$$

where

$$
\begin{aligned}
\bar{H}_1 &= -\varepsilon\Big(3(k_1 + k_2) - \big(p\beta_I + (1-p)\beta_A\big)\Big), \\
\bar{H}_2 &= -\varepsilon\big(p\varepsilon(\beta_A + \beta_I) + k_1 - 2p\beta_I\big), \\
\bar{H}_3 &= -\varepsilon\big(k_2 + \varepsilon(\beta_A + \beta_I) - p\beta_I\big), \\
\bar{H}_4 &= -\varepsilon\big(k_1 + k_2 + \varepsilon(\beta_A + \beta_I) - p\beta_I - (1-p)\beta_A\big).
\end{aligned}
$$

Accordingly, summing **Cases I** and **II** together and employing Lemma 3.3 can lead to globally asymptotically stable of $\mathcal{E}^*$ in $\mathring{\Omega}$. □

4 Numerical Results

In this section, the numerical solutions are simulated using Matlab with Runge-Kutta order 4 method.

4.1 Stability of equilibrium points

The stability of the model is studied by observing the solution's behaviors in Model (6). The numerical solutions are simulated by the following parameters from Table 1. We modify only β_I to 0.12 and β_A to 0.15 so that the value of $R_0 = 0.8238$ which less than one. In the biological meaning of $R_0 < 1$, the contact rate of each infected individual to other persons is less than one. Thus, the disease disappears from the area when time increases. The numerical solutions are depicted in Figure 2. It can be observed that the number of symptomatic and asymptomatic infected individuals decreases to zero. The number of recovered individuals initially increases and then decreases to zero. Susceptible individuals have been decrease to a constant value greater than zero. The simulation is consistent with Theorem 3.1.

Table 1: The description and values of parameters of the $SIAR$ model (6).

Parameter	Value	Unit	References
Π	2500	Days^{-1}	Assumed
β_I	0.4	-	[33]
β_A	0.4	-	[33]
p	0.602	-	[33]
μ	$1/(77 \times 365)$	Days^{-1}	[21, 34]
γ_I	$1/7$	Days^{-1}	[24]
γ_A	$1/5$	Days^{-1}	[24]
σ	0.25	Days^{-1}	Assumed
α	0.000015	Days^{-1}	Assumed

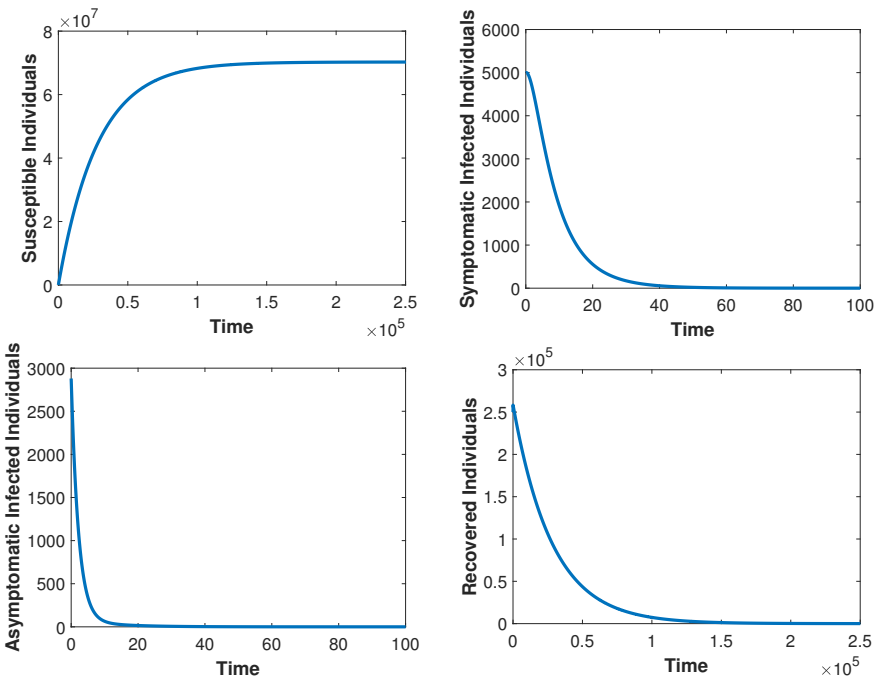

Figure 2: The simulations of the Model (6) for the case $R_0 = 0.8236$.

Regarding the stability of the endemic equilibrium, the numerical solutions are simulated using parameters exactly as shown in Table 1, resulting in $R_0 = 2.6576$. This means each infected individual can spread disease to more than one individual, indicating that the disease remains in the area. Numerical solutions are shown in Figure 3. It can be observed that the number of symptomatic infected and asymptomatic infected individuals reaches a maximum at the first peak and decrease to equilibrium points. Further, the number of susceptible and recovered individuals increase to the equilibrium point. This simulation is consistent with Theorem 3.2.

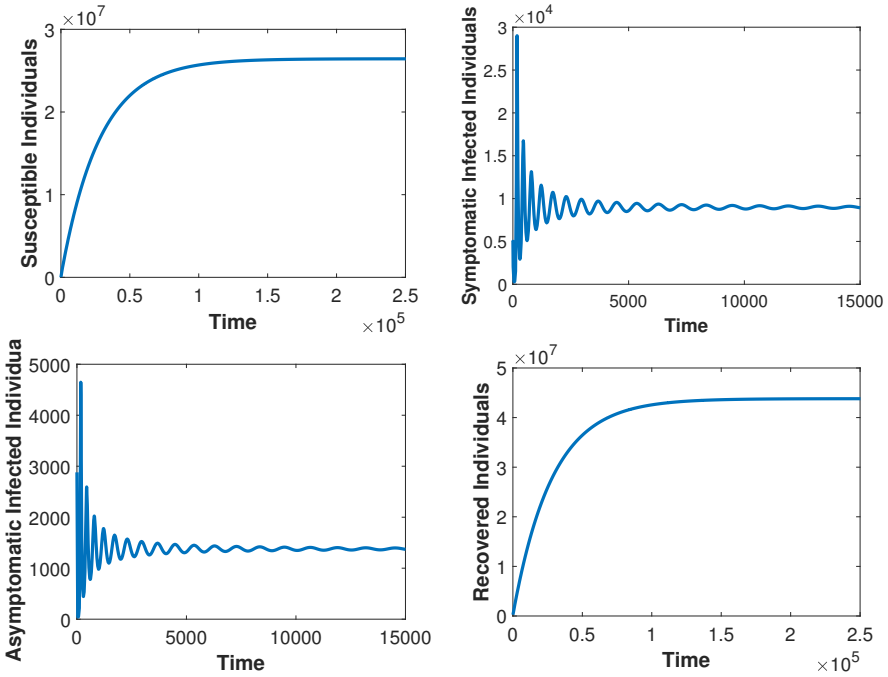

Figure 3: The simulations of the Model (6) for the case $R_0 = 2.6576$.

4.2 Numerical simulations for comparison SIAR model and infected cases of influenza A (H1N1) 2022 in Thailand

The Department of Disease Control started monitoring a new strain of influenza A (H1N1) on May 1, 2009, and found the first patient in Thailand toward the end of May. Subsequently, the number of patients increased, and the disease began to spread widely by June. The surveillance and monitoring program has concluded that in 2009 there were a total of $30,956$ patients with an infection rate of 48.78 per $100,000$ residents. Males are infected more than females at a ratio of $1.03 : 1$. There were 157 deaths, resulting in a death rate of 0.31 per $100,000$ residents, and a death-to-case ratio of 0.64. A significant number of patients were infected during the rainy season from June to September, reflecting the same trend as seasonal influenza. The central region has the highest infection among all regions of Thailand. Among occupations, students have the highest infection rate [29].

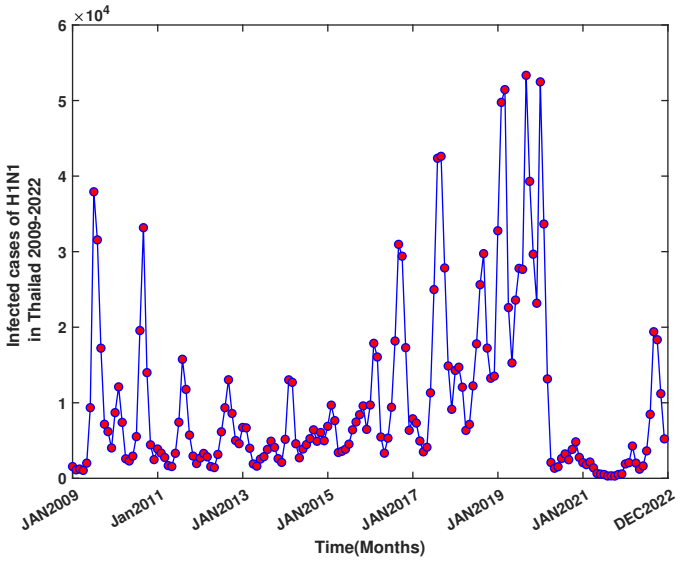

Figure 4: Number of monthly influenza A (H1N1) patients between 2009 – 2022.

Department of Disease Control, Ministry of Public Health have monitored monthly cases on the new influenza A (H1N1) strain from 2009 – 2022 [23] as shown Figure 4. In 2020, the reported cases irregularly decreased due to the COVID-19 epidemic in Thailand. Prevention guidelines and measures relevant to COVID-19 including social distancing, work from home policies, wearing masks and hand washing also helped prevent influenza infection due to similar transmission mechanisms. In 2022, the number of cases for the new strain influenza started to rise to previous levels as COVID-19 cases decreased due to mass vaccination in the country.

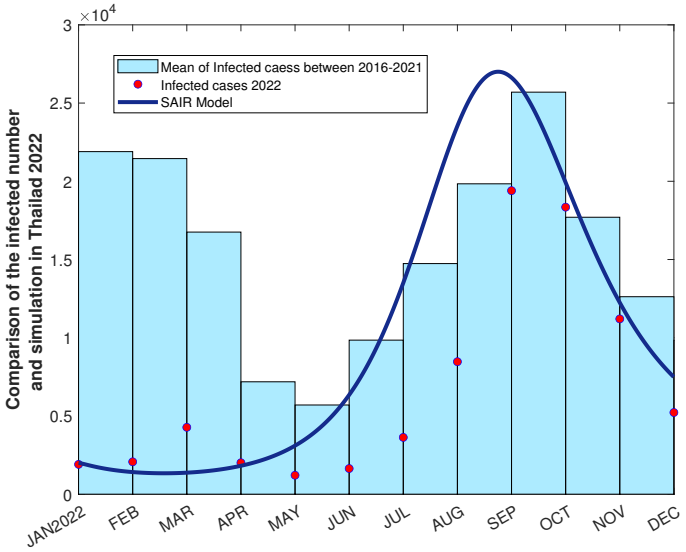

Figure 5: Comparison of the SIAR model and actual data of number of influenza A (H1N1) cases in 2022.

To validate our model, we run a simulation with the parameters shown in Table 1 for the year

2022 and compareed the results with real data. The reproduction number is 2.6576 $(R_0 > 1)$. As shown in Figure 5, our SIAR model successfully predicts the increasing trend in cases during the rainy season observed from June to September. It is noteworthy that this trend aligned with monthly average numbers of cases from $2016 - 2022$.

5 Sensitivity Analysis

This section investigates the impact of parameters on the dynamics of the Model (6). Sensitivity analysis is used to analyze these effects. We analyze sensitivity by using the values of parameters listed in Table 1 which are parameters utilized by Thai Department of Disease Control to predict the number of infected population from influenza A (H1N1) in Thailand.

5.1 Sensitivity analysis of R_0

In an epidemic model, disease outbreaks will increase or decrease depending on the value of basic reproduction number (R_0). If $R_0 > 1$, the outbreak continues to spread, while if $R_0 < 1$, the outbreak gradually decreased. Thus, it is crucial to identify the parameter which can reduce the value of R_0. This helps to design strategies to control disease outbreaks effectively. Sensitivity analysis of the basic reproduction number uses the normalized forward sensitivity index of a variable proposed in Nakul et al. [7, 32] by following the definition.

Definition 5.1. *The normalized forward sensitivity index of variable u that is differentiable with respect to parameter p is defined as:*

$$\Gamma_p^u := \frac{\partial u}{\partial p} \times \frac{p}{u}. \tag{24}$$

The sensitivity indices of R_0 is shown in Appendix A.

The sensitivity analysis of R_0 is analyzed by using parameter values in Table 1. The sensitivity indices of each parameter are calculated by the formula (24) and the results are shown in Table 2. From $\Gamma_{\beta_I}^{R_0} = +0.867$, it can be inferred that R_0 increases by 8.67% when β_I increases by 10%. Likewise, increasing parameters β_A, p and σ by 10%, results in the basic reproduction number R_0 increasing by 1.33%, 0.80% and 0.30%, respectively. Conversely, from $\Gamma_{\gamma_I}^{R_0} = -0.867$, in can be inferred that R_0 decreases by 8.67% when γ_I increases by 10%. Likewise, increasing γ_I, γ_A, μ and α by 10%, results in R_0 decreasing by 8.67%, 1.63%, 0.002% and 0.0009%, respectively.

Following the method outlined in [32], the relationship of parameters to the decrease of R_0 is summarized in Table 2. To reduce R_0 by 1%, it is necessary to increase parameters γ_I, γ_A, μ, and α individually by 1.14%, 5.99%, 4044.53%, and 10864.72%, respectively. Alternatively, decreasing parameters β_I, β_A, p, and σ by 1.15%, 7.51%, 12.42%, and 41.66%, respectively, would lead to the same reduction in R_0.

Table 2: Sensitivity indices of R_0 to parameters in model (6), evaluated at baseline parameter values in Table 1.

Parameters	Sensitivity index	Corresponding % change
β_I	$\Gamma_{\beta_I}^{R_0} = +0.86689$	-1.15355
β_A	$\Gamma_{\beta_A}^{R_0} = +0.13311$	-7.51264
p	$\Gamma_{p}^{R_0} = +0.08048$	-12.42474
σ	$\Gamma_{\sigma}^{R_0} = +0.02956$	-41.65959
γ_I	$\Gamma_{\gamma_I}^{R_0} = -0.86658$	$+1.14080$
γ_A	$\Gamma_{\gamma_A}^{R_0} = -0.16264$	$+5.98504$
μ	$\Gamma_{\mu}^{R_0} = -0.00024$	$+4044.53576$
α	$\Gamma_{\alpha}^{R_0} = -0.00009$	$+10864.72649$

Figure 6 shows the sensitivity indices of each parameter. It is evident that the most impactful parameters are β_I and γ_I followed by γ_A, β_A, p, σ, μ and α. This implies that the most efficient strategy for preventing the outbreak of influenza A (H1N1) is to either reduce the transmission rate from infected individuals or increase the recovery rate of infected individuals. These measures are the most efficient ways to mitigate the outbreak of H1N1 when the disease occurs.

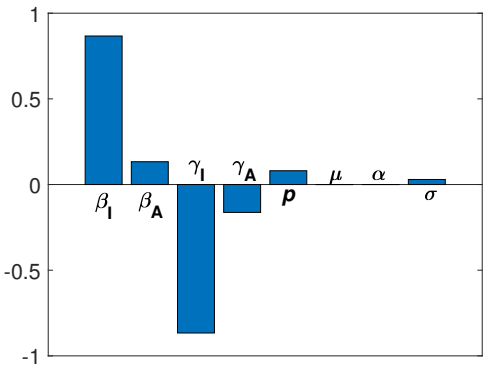

Figure 6: The sensitivity indices of R_0.

5.2 Sensitivity analysis of $\mathcal{E}^*$

In the epidemic model, endemic equilibrium ($\mathcal{E}^*$) represents the stable number of each subgroup of all individuals after the outbreak. An increase in outbreaks can be prevented if the number of infected individuals is reduced. Thus, it is important to identify parameters that help reduce the number of infected individuals. Sensitivity indices of $\mathcal{E}^*$ numerically calculated by the method in [7, 32] as shown in Appendix B.

The sensitivity indices of $\mathcal{E}^*$ are shown in Table 3. It can be observed that increasing Π has results in increasing the number of all individuals at the equilibrium because this parameter corresponds to the growth of the entire population. On the contrary, the number of all individuals decrease when μ increases because all individuals have a natural death rate of μ.

Table 3: Sensitivity indices of $\mathcal{E}^*$.

Parameters	**Endemic equilibrium**			
	S^*	I^*	A^*	R^*
Π	1.00000	1.00000	1.00000	1.00000
β_I	−0.86692	0.52295	0.52295	0.52295
β_A	−0.13311	0.08030	0.08030	0.08030
μ	−0.99976	−0.00042	−0.00023	−1.00038
σ	−0.02957	0.13723	−0.53768	0.01782
α	0.00004	−0.00013	−0.00002	−0.00011
γ_I	0.86667	−1.52245	−0.52280	−0.52251
γ_A	0.16265	−0.21749	−0.54253	−0.09807
p	−0.08050	0.37366	−1.46400	0.04852

The equilibrium of individuals I^*, A^* and R^* increases by increasing the parameters β_I and β_A while S^* decreases. On the contrary, the equilibrium of individuals I^*, A^* and R^* decreases by increasing parameters γ_I and γ_A while S^* increases.

This implies that following outbreaks of influenza A (H1N1), decreasing the transmission rate from symptomatic and asymptomatic infected individuals is the best measure to reduce the number of infected individuals at equilibrium. However, increasing the recovery rate in symptomatic and asymptomatic infected individuals appears to be the best measure to increase the susceptible individuals at equilibrium point.

Figure 7 shows a graph of the sensitivity indices of each parameter (except Π) of all subgroup individuals. The most sensitive parameter for S^* is μ followed by $\beta_I, \gamma_I, \gamma_A, \beta_A, p, \sigma$ and α, respectively. The most sensitive parameter for I^* is γ_I followed by $\beta_I, p, \gamma_A, \sigma, \mu$ and α. The most sensitive parameter for A^* is p followed by $\gamma_A, \beta_I, \sigma, \gamma_I, \beta_A, \mu$ and α. The most sensitive parameter for R^* is μ followed in order by $\beta_I, \gamma_I, \gamma_A, \beta_A, p, \sigma$ and α.

According to the results in Table 3 and Figure 7, the number of infected individuals decreases as the infected individual's recovered rate (γ_I) increases. This implies that early treatment will greatly reduce the number of infected individuals. Similarly, as the recovery rate of asymptomatic infected individuals (γ_A) increases, the number of asymptotic infected individuals decreases. Furthermore, decreasing the proportion of susceptible individuals who progress to symptomatic infected individuals (p) would result in better outbreak control for the number of asymptomatic infected individuals. Therefore, the key factors in controlling influenza H1N1 are not only controlling the spread of the disease (β_I and β_A), but also reducing the treatment time for patients in both individuals (γ_I and γ_A). However, during the H1N1 outbreak, wearing masks is the best way to protect ourselves, as is frequently checking our hands with alcohol gel, which will help reduce the risk of getting sick.

6 Conclusion

This research presented a SIAR model with constant immigration. The model has two equilibrium points: disease-free equilibrium ($\mathcal{E}_0$) and endemic equilibrium ($\mathcal{E}^*$). The global stability of $\mathcal{E}_0$ is analyzed by using the Lyapunov theorem, and $\mathcal{E}_0$ is globally asymptotically stable when

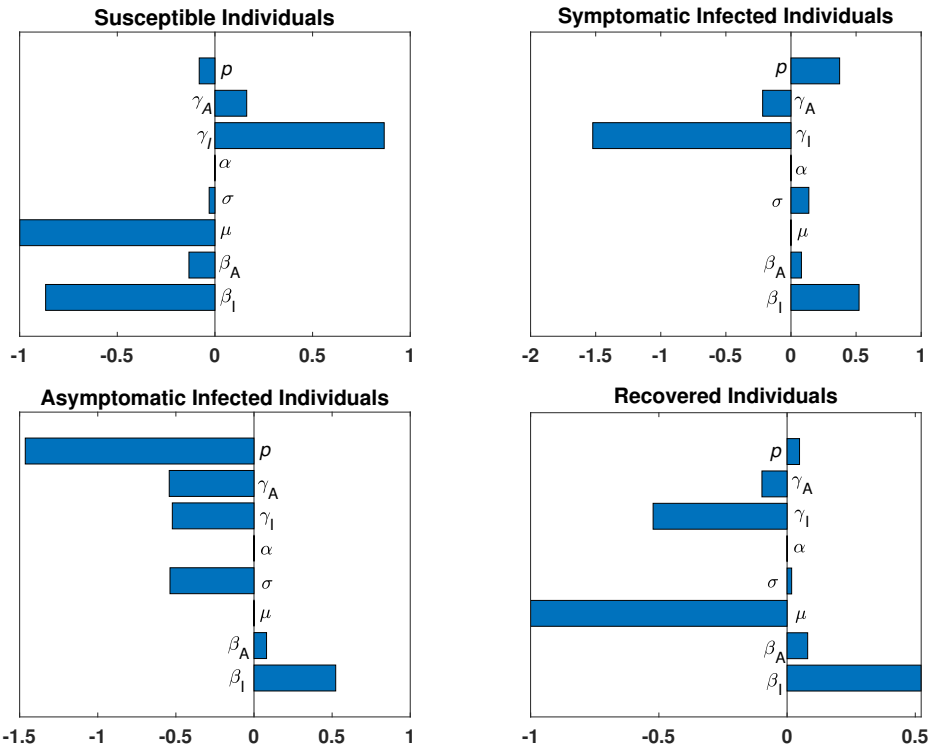

Figure 7: The sensitivity indices of endemic equilibrium ($\mathcal{E}^*$) in each individual.

$R_0 < 1$. By using the center manifold theorem, we shows that $\mathcal{E}^*$ is locally asymptotically stable when $R_0 > 1$. A geometric approach to global stability is applied to analyze the global stability of $\mathcal{E}^*$. For the case $\alpha = 0$ and under the conditions specified in Theorem 3.4, $\mathcal{E}^*$ is globally asymptotically stable when $R_0 > 1$.

The simulations of the Model (6) demonstrate that when $R_0 < 1$, the numerical solutions of the model approach to $\mathcal{E}_0$ as time increase. When $R_0 > 1$ solutions converge to $\mathcal{E}^*$, supporting the local stability theorem of equilibrium points. Furthermore, Model (6) is used to predict the trend of infected cases from influenza A (H1N1), as shown in Figure 5.

The sensitivity analysis of the basic reproduction number and the endemic equilibrium of the model are presented. The most sensitive parameters affecting the basic reproduction number are the transmission rate of symptomatic infected β_I and the recovery rate of symptomatic infected γ_I. The endemic equilibrium S^*, I^*, A^*, R^* are most sensitive to parameters Π ,γ_I, p and μ, respectively. Further, β_I and γ_I are the most effective parameters to reduce the number of infected individuals at the endemic equilibrium point. In conclusion, to prevent the disease, it is important to reduce the value of R_0. Thus, decreasing the transmission rate and increasing the recovery rate of the symptomatic infected individuals are the best strategies to prevent the disease. Furthermore, a decreasing transmission rate from infected β_I, and an increasing recovery rate in infected individuals γ_I are the best measures during a large outbreak.

Acknowledgement The author is very grateful to many people who read the manuscript and shared their valuable comments and suggestions, which helped improve the paper in the future. This research was funded by College of Industrial Technology, King Mongkut's University of Tech-

nology North Bangkok (Grant No. Res CIT0324/2018).

Conflicts of Interest The authors declare no conflict of interest.

References

[1] M. A. Abdoon, R. Saadeh, M. Berir, F. E. Guma & M. Ali (2023). Analysis, modeling and simulation of a fractional-order influenza model. *Alexandria Engineering Journal*, *74*, 231–240. https://doi.org/10.1016/j.aej.2023.05.011.

[2] S. M. Al-Zahrani, F. E. I. Elsmih, K. S. Al-Zahrani & S. Saber (2022). A fractional order SITR model for forecasting of transmission of COVID-19: sensitivity statistical analysis. *Malaysian Journal of Mathematical Sciences*, *16*(3), 517–536. https://doi.org/10.47836/mjms.16.3.08.

[3] S. Annas, M. I. Pratama, M. Rifandi, W. Sanusi & S. Side (2020). Stability analysis and numerical simulation of SEIR model for pandemic COVID-19 spread in indonesia. *Chaos, Solitons & Fractals*, *139*, Article ID: 110072. https://doi.org/10.1016/j.chaos.2020.110072.

[4] C. Castillo-Chavez & B. Song (2004). Dynamical models of tuberculosis and their applications. *Mathematical Biosciences & Engineering*, *1*(2), 361–404. https://doi.org/10.3934/mbe.2004.1.361.

[5] Centers for Disease Control and Prevention. Types of influenza viruses. https://www.cdc.gov/flu/about/viruses/types.htm 2023. Accessed: 2024-05-12.

[6] Centers for Disease Control and Prevention. Influenza. https://www.cdc.gov/flu/about/?CDC_AAref_Val=https://www.cdc.gov/flu/about/keyfacts.htm 2024. Accessed: 2024-05-13.

[7] N. Chitnis, J. M. Hyman & J. M. Cushing (2008). Determining important parameters in the spread of Malaria through the sensitivity analysis of a mathematical model. *Bulletin of Mathematical Biology*, *70*, 1272–1296. https://doi.org/10.1007/s11538-008-9299-0.

[8] I. Cooper, A. Mondal & C. G. Antonopoulos (2020). A SIR model assumption for the spread of COVID-19 in different communities. *Chaos, Solitons & Fractals*, *139*, Article ID: 110057. https://doi.org/10.1016/j.chaos.2020.110057.

[9] H. I. Freedman, S. Ruan & M. Tang (1994). Uniform persistence and flows near a closed positively invariant set. *Journal of Dynamics and Differential Equations*, *6*, 583–600. https://doi.org/10.1007/BF02218848.

[10] Z. Haque, M. Kamrujjaman, M. S. Alam & M. H. A. Biswas (2024). Marburg virus and risk factor among infected population: A modeling study. *Malaysian Journal of Mathematical Sciences*, *18*(1), 141–165. https://doi.org/10.47836/mjms.18.1.09.

[11] J. M. Jonnalagadda (2022). Epidemic analysis and mathematical modelling of H1N1 (A) with vaccination. *Nonautonomous Dynamical Systems*, *9*(1), 1–10. https://doi.org/10.1515/msds-2020-0143.

[12] C. W. Kanyiri, K. Mark & L. Luboobi (2018). Mathematical analysis of influenza A dynamics in the emergence of drug resistance. *Computational and Mathematical Methods in Medicine*, *2018*(1), Article ID: 2434560. https://doi.org/10.1155/2018/2434560.

[13] F. Khondaker (2022). Optimal control analysis of influenza epidemic model. *Applied Mathematics*, *13*(10), 845–857. https://doi.org/10.4236/am.2022.1310053.

[14] Y. Kim, A. V. Barber & S. Lee (2020). Modeling influenza transmission dynamics with media coverage data of the 2009 H1N1 outbreak in Korea. *PLOS One*, *15*(6), e0232580. https://doi.org/10.1371/journal.pone.0232580.

[15] J. P. La Salle (1976). *The Stability of Dynamical Systems*. CBMS-NSF Regional Conference Series in Applied Mathematics. SIAM Society for Industrial and Applied Mathematics, Philadelphia. https://doi.org/10.1137/1.9781611970432.

[16] M. Y. Li, J. R. Graef, L. Wang & J. Karsai (1999). Global dynamics of a SEIR model with varying total population size. *Mathematical Biosciences*, *160*(2), 191–213. https://doi.org/10.1016/S0025-5564(99)00030-9.

[17] M. Y. Li & J. S. Muldowney (1996). A geometric approach to global-stability problems. *SIAM Journal on Mathematical Analysis*, *27*(4), 1070–1083. https://doi.org/10.1137/S0036141094266449.

[18] M. Y. Li & J. S. Muldowney (2000). Dynamics of differential equations on invariant manifolds. *Journal of Differential Equations*, *168*(2), 295–320. https://doi.org/10.1006/jdeq.2000.3888.

[19] S. Liu, Y. Bi & Y. Liu (2020). Modeling and dynamic analysis of tuberculosis in mainland China from 1998 to 2017: The effect of DOTS strategy and further control. *Theoretical Biology and Medical Modelling*, *17*(1), 6. https://doi.org/10.1186/s12976-020-00124-9.

[20] G. Lu & Z. Lu (2017). Geometric approach to global asymptotic stability for the SEIRS models in epidemiology. *Nonlinear Analysis: Real World Applications*, *36*, 20–43. https://doi.org/10.1016/j.nonrwa.2016.12.005.

[21] Macrotrends. Thailand life expectancy 1950-2023. https://www.macrotrends.net/countries/THA/thailand/life-expectancy 2009. Accessed: 2023-12-25.

[22] A. Malik, M. Alkholief, F. M. Aldakheel, A. A. Khan, Z. Ahmad, W. Kamal, M. K. Gatasheh & A. Alshamsan (2022). Sensitivity analysis of COVID-19 with quarantine and vaccination: A fractal-fractional model. *Alexandria Engineering Journal*, *61*(11), 8859–8874. https://doi.org/10.1016/j.aej.2022.02.024.

[23] Ministry of Public Health, Department of Disease Control. Weekly disease forecast. https://ddc.moph.go.th/en/index.php 2009. Accessed: 2023-12-25.

[24] Ministry of Public Health, Department of Disease Control. Influenza (A). https://ddc.moph.go.th/disease_detail.php?d=20 2022. Accessed: 2022-12-01.

[25] Ministry of Public Health, Department of Disease Control. Influenza, flu. https://ddc.moph.go.th/disease_detail.php?d=13 2022. Accessed: 2024-13-05.

[26] Ministry of Public Health, Department of Disease Control. Weekly disease forecast. https://ddc.moph.go.th/doe/pagecontent.php?page=607&dept=doe 2023. Accessed: 2023-10-1.

[27] S. Mwalili, M. Kimathi, V. Ojiambo, D. Gathungu & R. Mbogo (2020). SEIR model for COVID-19 dynamics incorporating the environment and social distancing. *BMC Research Notes*, *13*(1), Article ID: 352. https://doi.org/10.1186/s13104-020-05192-1.

[28] S. Ottaviano, M. Sensi & S. Sottile (2022). Global stability of sairs epidemic models. *Nonlinear Analysis: Real World Applications*, *65*, Article ID: 103501. https://doi.org/10.1016/j.nonrwa.2021.103501.

[29] Pediatric Infectious Disease Society of Thailand. Influenza. https://www.pidst.or.th/A223.html 2024. Accessed: 2024-05-20.

[30] Y. M. Rangkuti, Firmansyah & A. Landong (2022). Sensitivity analysis of SEIR epidemic model of COVID-19 spread in Indonesia. In *Journal of Physics: Conference Series*, volume 2193 pp. Article ID: 012092. IOP Publishing. https://dx.doi.org/10.1088/1742-6596/2193/1/012092.

[31] I. Ratti & P. Kalra (2023). Study of disease dynamics of co-infection of rotavirus and Malaria with control strategies. *Malaysian Journal of Mathematical Sciences*, *17*(2), 151–177. https://doi.org/10.47836/mjms.17.2.05.

[32] M. Samsuzzoha, M. Singh & D. Lucy (2013). Uncertainty and sensitivity analysis of the basic reproduction number of a vaccinated epidemic model of influenza. *Applied Mathematical Modelling*, *37*(3), 903–915. https://doi.org/10.1016/j.apm.2012.03.029.

[33] X. Tan, L. Yuan, J. Zhou, Y. Zheng & F. Yang (2013). Modeling the initial transmission dynamics of influenza A H1N1 in Guangdong Province, China. *International Journal of Infectious Diseases*, *17*(7), e479–e484. https://doi.org/10.1016/j.ijid.2012.11.018.

[34] World Health Organization. Thailand (Statistics). https://www.who.int/countries/tha/ 2019. Accessed: 2024-05-6.

[35] World Health Organization. Influenza A (H1N1) outbreak. https://www.who.int/emergencies/situations/influenza-a-(h1n1)-outbreak 2024. Accessed: 2024-05-20.

APPENDIX

A Sensitivity Indices of R_0

Substitute $k_1 = \mu + \alpha + \gamma_I$ and $k_2 = \mu + \sigma + \gamma_A$ in (8), the basic reproduction number R_0 is rewritten in form,

$$R_0 = \frac{p\beta_I(\mu + \gamma_A + \sigma) + (1-p)\big(\beta_I\sigma + \beta_A(\mu + \gamma_I + \alpha)\big)}{(\mu + \gamma_I + \alpha)(\mu + \gamma_A + \sigma)}.$$

Thus, the sensitivity indices of R_0 based on 8 parameters as show in following,

$$\begin{aligned}
\Gamma_{\beta_I}^{R_0} &= \frac{\beta d_I\big(pk_2 + (1-p)\sigma\big)}{p\beta_I k_2 + (1-p)(\beta_I\sigma + \beta_A k_1)},\\
\Gamma_{\beta_A}^{R_0} &= \frac{(1-p)\beta_A k_1}{p\beta_I k_2 + (1-p)(\beta_I\sigma + \beta_A k_1)},\\
\Gamma_{\gamma_I}^{R_0} &= \frac{\gamma_I\big((1-p)\beta_A k_1 - p\beta_I k_2 - (1-p)(\beta_I\sigma + \beta_A k_1)\big)}{k_1\big(p\beta_I k_2 + (1-p)(\beta_I\sigma + \beta_A k_1)\big)},\\
\Gamma_{\gamma_A}^{R_0} &= \frac{-\gamma_A(1-p)(\beta_I\sigma + \beta_A k_1)}{k_2\big(p\beta_I k_2 + (1-p)(\beta_I\sigma + \beta_A k_1)\big)},\\
\Gamma_{\sigma}^{R_0} &= \frac{\sigma\big((1-p)\beta_I k_2 - (1-p)(\beta_I\sigma + \beta_A k_1)\big)}{k_2\big(p\beta_I k_2 + (1-p)(\beta_I\sigma + \beta_A k_1)\big)},\\
\Gamma_{p}^{R_0} &= \frac{pk_1k_2}{p\beta_I k_2 + (1-p)(\beta_I\sigma + \beta_A k_1)},\\
\Gamma_{\mu}^{R_0} &= \frac{\mu\Big(\big(p\beta_I + (1-p)\beta_A\big)k_1k_2 - (k_1+k_2)\big(p\beta_I k_2 + (1-p)(\beta_I\sigma + \beta_A k_1)\big)\Big)}{k_1k_2\big(p\beta_I k_2 + (1-p)(\beta_I\sigma + \beta_A k_1)\big)},\\
\Gamma_{\alpha}^{R_0} &= \frac{\alpha\Big((1-p)\beta_A k_1 - \big(p\beta_I k_2 + (1-p)(\beta_I\sigma + \beta_A k_1)\big)\Big)}{k_1\big(p\beta_I k_2 + (1-p)(\beta_I\sigma + \beta_A k_1)\big)}.
\end{aligned}$$

B Sensitivity Indices of $\mathcal{E}^*$

The four state variables at the endemic equilibrium point (S, I, A, R) are denoted by x_1, x_2, x_3, x_4 and the nine parameters $(\Pi, \beta_I, \ldots, \alpha)$ are notation by $p_1, p_2, \ldots, p_9$ and four equilibrium equations of (6) by,

$$\begin{aligned}
g_1(x_1,\ldots,x_4;p_1,\ldots,p_9) &= p_1 - \frac{(x_2p_2 + x_3p_3)x_1}{x_1+x_2+x_3+x_4} - p_4x_1 = 0,\\
g_2(x_1,\ldots,x_4;p_1,\ldots,p_9) &= \frac{p_9(x_2p_2 + x_3p_3)x_1}{x_1+x_2+x_3+x_4} + p_5x_3 - (p_4+p_6+p_7)x_2 = 0,\\
g_3(x_1,\ldots,x_4;p_1,\ldots,p_9) &= \frac{(1-p_9)(x_2p_2 + x_3p_3)x_1}{x_1+x_2+x_3+x_4} - (p_4+p_5+p_8)x_3 = 0,\\
g_4(x_1,\ldots,x_4;p_1,\ldots,p_9) &= x_2p_7 + x_3p_8 - x_4p_4 = 0.
\end{aligned} \tag{25}$$

Following the condition $\partial p_l/\partial p_j = 0$ when $l \neq j$, full derivatives of (25) with respect to the nine parameters, p_j are shown in the form,

$$AX_j = K_j,$$

where

$$A = \begin{bmatrix} a_{11} & a_{12} & a_{13} & a_{14} \\ a_{21} & a_{22} & a_{23} & a_{24} \\ a_{31} & a_{32} & a_{33} & a_{34} \\ a_{41} & a_{42} & a_{43} & a_{44} \end{bmatrix}; \quad X_j = \begin{bmatrix} \partial x_1^*/\partial p_j \\ \partial x_2^*/\partial p_j \\ \partial x_3^*/\partial p_j \\ \partial x_4^*/\partial p_j \end{bmatrix}; \quad K_j = \begin{bmatrix} -\partial g_1/\partial p_j \\ -\partial g_2/\partial p_j \\ -\partial g_3/\partial p_j \\ -\partial g_4/\partial p_j \end{bmatrix},$$

$$\begin{aligned}
a_{11} &= -\frac{p_2x_2 + p_3x_3}{x_1 + x_2 + x_3 + x_4} + \frac{(p_2x_2 + p_3x_3)x_1}{(x_1 + x_2 + x_3 + x_4)^2} - p_4, \\
a_{12} &= -\frac{p_2x_1}{x_1 + x_2 + x_3 + x_4} + \frac{(p_2x_2 + p_3x_3)x_1}{(x_1 + x_2 + x_3 + x_4)^2}, \\
a_{13} &= -\frac{p_3x_1}{x_1 + x_2 + x_3 + x_4} + \frac{(p_2x_2 + p_3x_3)x_1}{(x_1 + x_2 + x_3 + x_4)^2}, \\
a_{14} &= \frac{(p_2x_2 + p_3x_3)x_1}{(x_1 + x_2 + x_3 + x_4)^2}, \\
a_{21} &= \frac{p_9(p_2x_2 + p_3x_3)}{x_1 + x_2 + x_3 + x_4} - \frac{p_9(p_2x_2 + p_3x_3)x_1}{(x_1 + x_2 + x_3 + x_4)^2}, \\
a_{22} &= \frac{p_2p_9x_1}{x_1 + x_2 + x_3 + x_4} - \frac{p_9(p_2x_2 + p_3x_3)x_1}{(x_1 + x_2 + x_3 + x_4)^2} - p_4 - p_6 - p_7, \\
a_{23} &= \frac{p_3p_9x_1}{x_1 + x_2 + x_3 + x_4} - \frac{p_9(p_2x_2 + p_3x_3)x_1}{(x_1 + x_2 + x_3 + x_4)^2} + p_5, \\
a_{24} &= -\frac{p_9(p_2x_2 + p_3x_3)x_1}{(x_1 + x_2 + x_3 + x_4)^2}, \\
a_{31} &= \frac{(1 - p_9)(p_2x_2 + p_3x_3)}{x_1 + x_2 + x_3 + x_4} - \frac{(1 - p_9)(p_2x_2 + p_3x_3)x_1}{(x_1 + x_2 + x_3 + x_4)^2}, \\
a_{32} &= \frac{(1 - p_9)p_2x_1}{x_1 + x_2 + x_3 + x_4} - \frac{(1 - p_9)(p_2x_2 + p_3x_3)x_1}{(x_1 + x_2 + x_3 + x_4)^2}, \\
a_{33} &= \frac{(1 - p_9)p_3x_1}{x_1 + x_2 + x_3 + x_4} - \frac{(1 - p_9)(p_2x_2 + p_3x_3)x_1}{(x_1 + x_2 + x_3 + x_4)^2} - p_4 - p_5 - p_8, \\
a_{34} &= -\frac{(1 - p_9)(p_2x_2 + p_3x_3)x_1}{(x_1 + x_2 + x_3 + x_4)^2}, \\
a_{41} &= 0, \quad a_{42} = p_7, \quad a_{43} = p_8, \quad a_{44} = -p_4.
\end{aligned}$$

Sensitivity indices of endemic equilibrium x_i^* to parameter p_j is denoted by,

$$\frac{\partial x_i^*}{\partial p_j} \cdot \frac{p_j}{x_i^*},$$

where $1 \leq i \leq 4$ and $1 \leq j \leq 9$.